

**HSP90: COMMON TARGET FOR DIVERSE
ANTIBIOTICS**

Palgunan Kalyanaraman

Master of Science
University of Madras
Chennai, India
2001

Submitted to the Faculty of the
Graduate College of the
Oklahoma State University
in partial fulfillment of
the requirements for
the Degree of
MASTER OF SCIENCE
December 2006

**HSP90: COMMON TARGET FOR DIVERSE
ANTIBIOTICS**

Thesis Approved:

Dr. Robert L. Matts (Chairman)

Dr. Steve D. Hartson (Advisor)

Dr. Richard C. Essenberg

Dean Graduate College

ACKNOWLEDGEMENTS

This thesis would not have been possible without the co-operation, support and blessing of many individuals. I would like to express my gratitude to those who helped in this accomplishment. I would like to dedicate this thesis to my father, grandmother and the best friend of mine Sunil, without their blessings I could not have accomplished anything.

First and foremost, I would like to thank Dr. Steve D.Hartson, for giving me an opportunity to work in this project and help me pursue my Masters degree in his lab. I would be running out of space if I start talking about the encouragement, guidance, and kindness shown towards me. In the time of great losses and personal tragedy in my life, he has been a comforter and motivator, without his words I could not have come this far.

I sincerely thank Dr. Robert L. Matts for his guidance and support. I am equally grateful to him, for allowing me to work in his lab and for his patience and invaluable suggestions at the time I needed them the most. I thank Dr. Richard C. Essenberg for opening the gateway for me to enter Oklahoma state university. He has helped me in extending my admission status at OSU, without which I would not have been able to transfer from city college of New York.

I owe a lot to my colleagues Letong Jia, Jeannie Te, Amy Hurst, Yixing Wang for being a great research partners and friends. I feel myself to be luckiest guy to get a friend like Ashok Rajendran, who has been supportive from my undergraduate college. I thank Palaniappan Chetty, Meena, Vijay Ramakrishnan and Balaji Hariharasundaram for their encourage and support.

Most of all, I wish to thank my aunt, uncle and mother for their love and support. I thank my brother for his motivation and encouragement. They are the people whom I look upon for courage and hard work.

TABLE OF CONTENTS

Chapter.....	Pages
1. INTRODUCTION.....	1
Protein folding and molecular chaperones.....	1
Reasons and consequences of protein misfolding.....	1
Protein folding requires molecular chaperones.....	2
Heat shock protein90 (Hsp90).....	3
Domain structure of Hsp90.....	4
Carboxy-termian domain of Hsp90.....	5
Crystal structure of the carboxy terminal domain of <i>E. coli</i> (HtpG).....	5
Conformational states of Hsp90.....	8
Geldanamycin and molybdate inhibit Hsp90's ATPase cycle.....	10
Novobiocin inhibits Hsp90 function.....	12
Other natural compounds may inhibit Hsp90.....	14
2. Materials and Methods	
Preparation of reagents.....	16
Preparation of wash buffers.....	17
Purification and protease finger printing of recombinant Hsp90.....	17
Protease fingerprinting of Hsp90.....	18
Analysis of the effects of drugs on Hsp90-substrate interactions.....	18
Kinase activity of Lck.....	19

3.	Curcumin, epigallocatechin gallate and novobiocin inhibit Hsp90-dependent folding of Lck.....	21
	Curcumin, epigallocatechin gallate and novobiocin do not inhibit Lck directly.....	24
	Effect of curcumin,epigallocateching allate and novobicoicn on the interaction of Lck and Hsp90.....	26
	Effect of curcumin,epigallocatechin gallate and novobiocin on the Interaction of mature Lck with Hsp90.....	28
	Molybate and geldanamycin have opposite effects on Hsp90.....	30
	Effect of novobiocin on the conformation of Hsp90.....	33
	Novobiocin reverses molybdate induced conformational changes on the C-terminal domain of full-length Hsp90.....	35
	Effect of epigallocatechin gallate on the conformation of Lck.....	37
	Effect of curcumin on the conformation of Lck.....	39
	Curcumin and geldanamycin do not compete for same binding site on Hsp90.....	41
	Curcumin and epigallocatechin gallate do not compete for same binding site on Hsp90.....	43
	Curcumin and novobiocin do not compete for same binding site on Hsp90.....	45
	Novobiocin, curcumin, epigallocatechin gallate do not inhibit trypsin.....	47

	Novobiocin protects carboxy terminus of Hsp90 from cleavage by trypsin.....	49
	Epigallocatechin gallate protects carboxy terminus of Hsp90 from cleavage by trypsin.....	51
	Curcumin gallate protects carboxy terminus of Hsp90 from cleavage by trypsin.....	53
4	Discussion.....	55
5	Introduction.....	70
	Novobiocin binds to the carboxy terminus of Hsp90.....	70
	Novobiocin inhibits co-chaperone binding to Hsp90.....	70
	Materials and Methods.....	71
	Reagents.....	71
	UV crosslinking.....	71
	Results.....	74
	Photoexposure of novobiocin to Hsp90-CT.....	74
	Photoaffinity analogs.....	76
	Photoexposure (UV) of Hsp90-CT and <i>KU-26</i>	78
	Crosslinking of novobiocin analogs to Hsp90-CT is highly specific.....	81
	Discussion.....	83
	Bibliography.....	85

ABBREVIATIONS

ADP	adenosine diphosphate
AHA1	activator of Hsp90 ATPase homologue 1
ATP	adenosine triphosphate
CC	curcumin
DNA	deoxyribonucleic acid
DMSO	dimethyl sulfoxide
DTT	dithiothretol
EDTA	ethylenediaminetetraacetic acid
EG	epigallocatechin gallate
GA	geldanamycin
HEPES	4-(2-Hydroxyethyl)piperazine-1-ethanesulfonic acid
HRI	heme-regulated inhibitor of protein synthesis
Hsp	heat shock proteins
Hsp90-CT	carboxy terminal domain of Hsp90.
HtpG	high temperature protein G
KDa	kilo dalton
KAM	kinase assay mix
KU	university of kansas
Lck	lymphoid cell kinase
μl	micro liter

mM	milli molar
MoO ₄	molybdate
MALDI-TOF	matrix assisted laser desorption/ionization-time of flight
NB	novobiocin
Pi	phosphate
PIPES	piperazine-N,N' -bis[2-ethanesulfonic acid]
PVDF	polyvinylidene difluoride
RRL	rabbit reticulocyte lysate
SDS-PAGE	sodium dodecyl sulfate-polyacrylamide gel electrophoresis
Src	rous sarcoma virus oncogene
TnT	invitro transcription and translation
TPR	tetratricopeptide repeats
UV	ultraviolet

LIST OF FIGURES

1	Domain organization of Human Hsp90 α	4
2	Crystal structure of C-terminal domain of Hsp90	7
3	The open and closed conformation of Hsp90	10
4	Model of ATPase cycle of Hsp90	11
5	Structure of ATP and novobiocin	13
6	Structure of epigallocatechin gallate	14
7	Structure of curcumin	15
8	Effect of curcumin, epigallocatechin gallate, novobiocin and geldanamycin on Hsp90-mediated folding of Lck	23
9	Curcumin, epigallocatechin gallate and novobiocin do not inhibit kinase directly	25
10	Effect of curcumin, epigallocatechin gallate and novobiocin on interaction of Lck and Hsp90 in RRL	27
11	Curcumin, epigallocatechin galalte and novobiocin do not inhibit kinase directly	29
12	Effect of molybdate and geldanamycin on structural conformation of Hsp90	32
13	Effect of novobiocin on structural conformation of Hsp90	34
14	Novobiocin reverses molybdate-induced conformational changes on the C-terminal domain of full-length Hsp90	36
15	Effect of epigallocatechin gallate on Hsp90 conformation	38
16	Curcumin has unique mechanism of action on Hsp90	40
17	Curcumin and geldanamycin do not compete for same binding site on Hsp90	42
18	Curcumin and epigallocatechin gallate do not compete for	44

	same binding site on Hsp90	
19	Curcumin and novobiocin do not compete for same binding site on Hsp90	46
20	Novobiocin, curcumin, epigallocatechin gallate do not inhibit trypsin	48
21	Novobiocin alters conformation of C-terminal domain of Hsp90	50
22	Epigallocatechin gallate alters conformation of C-terminal domain of Hsp90	52
23	Curcumin alters the conformation of C-terminal domain of Hsp90	54
24	Effect of molybdate and geldanamycin on Hsp90 ATPase cycle	61
25	Novobiocin mediates conformational changes on Hsp90	64
26	Effect of molybdate and novobiocin on Hsp90-ATPase cycle	66
27	Structure of photoaffinity analogs of novobiocin	73
28	Photoexposure of novobiocin and Hsp90-CT	75
29	Novobiocin analog <i>KU-26</i> alters the conformation of Hsp90-CT	77
30	Photoaffinity novobiocin analogs specifically crosslink to the C-terminal domain of Hsp90	79
31	Crosslinking of novobiocin analogs is highly specific	82

Chapter 1

INTRODUCTION

Literature Review: Protein folding and molecular chaperones

Newly synthesized proteins must fold to unique three dimensional structures to become functionally active. The native fold of protein is encoded in its amino acid sequence (1). One of the big challenges of modern science is to uncover the mechanism of protein folding (2). How the protein folds to a three dimensional structure is still unknown. Anfinsen et al (3) suggested that primary amino acid sequence of proteins has all the information to fold into a native conformation. However, the key to proper folding of proteins lie in the ability of hydrophobic amino acid side chains to shy away from aqueous environment to form an hydrophobic core (4). Proper folding of protein is essential for many biological processes such as directing molecules to specific cellular locations (1).

Reasons and consequences of protein misfolding

Single domain proteins can bury exposed hydrophobic amino acids residues rapidly after the initiation of folding (1, 6). However, multidomain proteins tend to fold inefficiently forming partially folded intermediates, which tend to aggregate. The primary reason for misfolding of proteins or aggregation of proteins occur due to exposure of hydrophobic amino acids residues to the solvent, leading to aggregation of proteins (1,6).

The formation of structured fibrillar aggregates are often related with diseases such as Alzheimer's or Huntington's (6, 7).

Protein folding requires molecular chaperones

Living systems have adapted themselves to tackle misfolding abnormalities caused in living cell (8, 9). The primary defense against aggregation comes from a set of proteins called molecular chaperones. Molecular chaperones helps in proper folding of newly synthesized proteins, preventing them from aggregation. Molecular chaperones ensure that correct folding is achieved in a highly crowded living cell (10). Molecular chaperones also have the ability rescue misfolded and aggregated proteins and make them functionally active (8, 9).

Most molecular chaperones are called stress proteins as they are induced by several other external factors such as heat shock, tissue damage, exposure of cells to detergents, heavy metals, infection etc., and (11). Stress proteins or Heat Shock Proteins (Hsp) ranges from molecular size 8 to 150 kDa. The stress proteins are classified into six major families Hsp100, Hsp90, Hsp70, Hsp60, Hsp 40 and some other small heat shock proteins.

Major molecular chaperones families have been studied and more extensive reviews of molecular chaperones are reported (12, 13, 14, 15, and 16). My thesis focuses on ability of drugs to alter the structure and function Hsp90. I will review the structure and function of Hsp90.

Heat shock protein 90 (Hsp90)

Heat shock protein 90 (Hsp90) is the most abundant protein present in cytosol; approximately 2% of the cytosolic protein content is Hsp90 (17). Hsp90 is present at all times in cytosol. It is induced further during stress (heat shock, etc.) (18).

Hsp90 is highly conserved, human Hsp90 having a 60% sequence homology with yeast and 40% homology with *E. coli*. Hsp90 exists in two highly similar isoforms in human cytosol (Hsp90 α and Hsp90 β). Hsp90 isoforms are also present in mitochondria (TRAP1) and in endoplasmic reticulum (Grp94). In bacterial cells, Hsp90 homologue is called HtpG (high temperature protein G).

Many proteins require Hsp90 for their proper function and are therefore called “clients” (24). These proteins include steroid hormone receptors and serine/threonine/tyrosine kinases (19). However, Hsp90’s ability to fold steroid hormone receptors is mainly due to its ability to involve other molecular chaperones in an ordered assembly pathway (16). Although, purified Hsp90 shows a weak interaction with variety of peptides (20, 21, and 22). Co-chaperones are the physical and functional partners of Hsp90.

Domain structure of Hsp90

Proteolytic studies and sequence alignments have been used to define the individual domains on Hsp90. Hsp90 has 3-4 domains, namely the N terminal domain, a charged linker region connecting the N terminal and the middle domain region of Hsp90, followed by the C terminal domain (Figure 1).

The crystal structure of Hsp90’s N-terminal domain was solved for human (23), yeast (24), and *E. coli* (25) homologs. The tertiary structure of the N terminal domain is

highly conserved between Hsp90 of *E. coli* (Htp G) and yeast (Hsp 82). Biochemical and crystallographic studies of the N terminal domain of Hsp90 (residues 1-232 in human) reveals a binding site for ATP/ADP. The N- terminus ATP binding site was also found to bind two Hsp90 inhibitors namely radicicol and geldanamycin (26, 27). Hsp90 function is primarily based on its ability to bind and hydrolyze ATP (28).

Eukaryotic have Hsp90 a charged linker region connecting the N terminal domain and middle domain of Hsp90. This region is very susceptible to proteolysis. This charged linker regions are rich in amino acids glutamic acid, aspartic acid and lysine (29). The charged region has been found to increase the ability of Hsp90 to bind to peptide and also found to establish a link between ATP and peptide binding to Hsp90 (30). The charged linker region is essential for Hsp90 chaperone activity.

Recent evidence suggests that the middle domain of Hsp90 was found to interact with newly identified protein called AHA1 (activator of Hsp90 ATPase homologue 1). This AHA1 promotes the association of N terminal and middle segment of Hsp90. This leads to a rapid hydrolysis of ATP (33, 34).

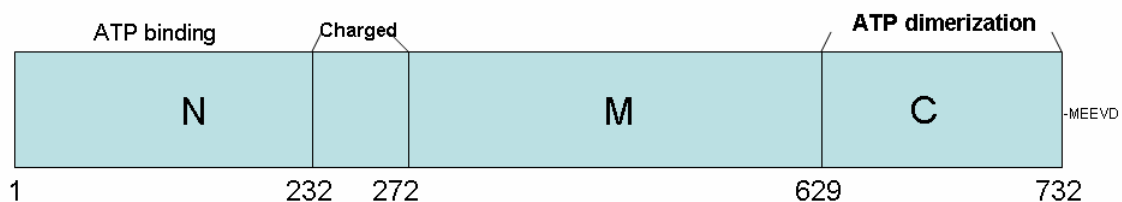


Figure 1: Domain organization of Human Hsp90α (34)

Carboxy-terminal domain of Hsp90

The carboxy-terminal domain of Hsp90 (residues 609-732) is important for dimerization of Hsp90 (34). The C terminal domain is thought to have a nucleotide binding site (35) also found to bind an antibiotic called novobiocin (35). The binding of ATP to the C terminus of Hsp90 requires the amino terminal nucleotide binding site to be occupied by ATP or geldanamycin (36). The C terminus of Hsp90 also contains a highly conserved MEEVD motif which is the binding site of Hsp90 co-chaperones containing tetratricopeptide repeats (TPR). The mammalian TPR co-chaperones include immunophilins (FKBP52, FKBP51), Hop/Sti, PP5, cyclophilin-40) (30, 37, 38).

In default conformation, Hsp90 dimerizes through its C-terminal domain. N-terminal ATP binding and hydrolysis to promote the transient interaction of two N-terminal domains leading to the formation of molecular clamp (28). The conformational cycle of Hsp90 is discussed in more detail below.

Crystal structure of the carboxy terminal domain of *E. coli* (HtpG).

The crystal structure of the carboxy terminal domain of *E. coli* Hsp90 (HtpG) reveals a potential drug binding pocket (Figure 2B) (36 “B”) because of the highly conserved nature of Hsp90 (*E. coli* HtpG has 40% sequence homology with human Hsp90), this crystal structure acts as a good template to study the drug-binding and nucleotide-binding sites on human Hsp90. In HtpG crystal structure, helix 4 and helix 5 act as a dimerization domain forming Hsp90 homodimer. The helix 4 also contains a hydrophobic motif (*E. coli* amino acid residues 653-669), which has the potential binding site of novobiocin.

Helix 2 forms another face of the hypothetical binding site of novobiocin. Even though the identity of hydrophobic residues differ from *E. coli* to human Hsp90 (601ANMERIMKA₆₀₈), the hydrophobic nature of helix 2 is preserved. In crystals the helix 2 is exposed to solvent. In protease nicking assays of the native protein, flexibility of this motif makes it vulnerable to trypsinolysis (Figure 2A). In our drug-binding studies, we observe that the binding of drugs to the C-terminal domain of Hsp90 induces structural and functional changes on Hsp90 (25).

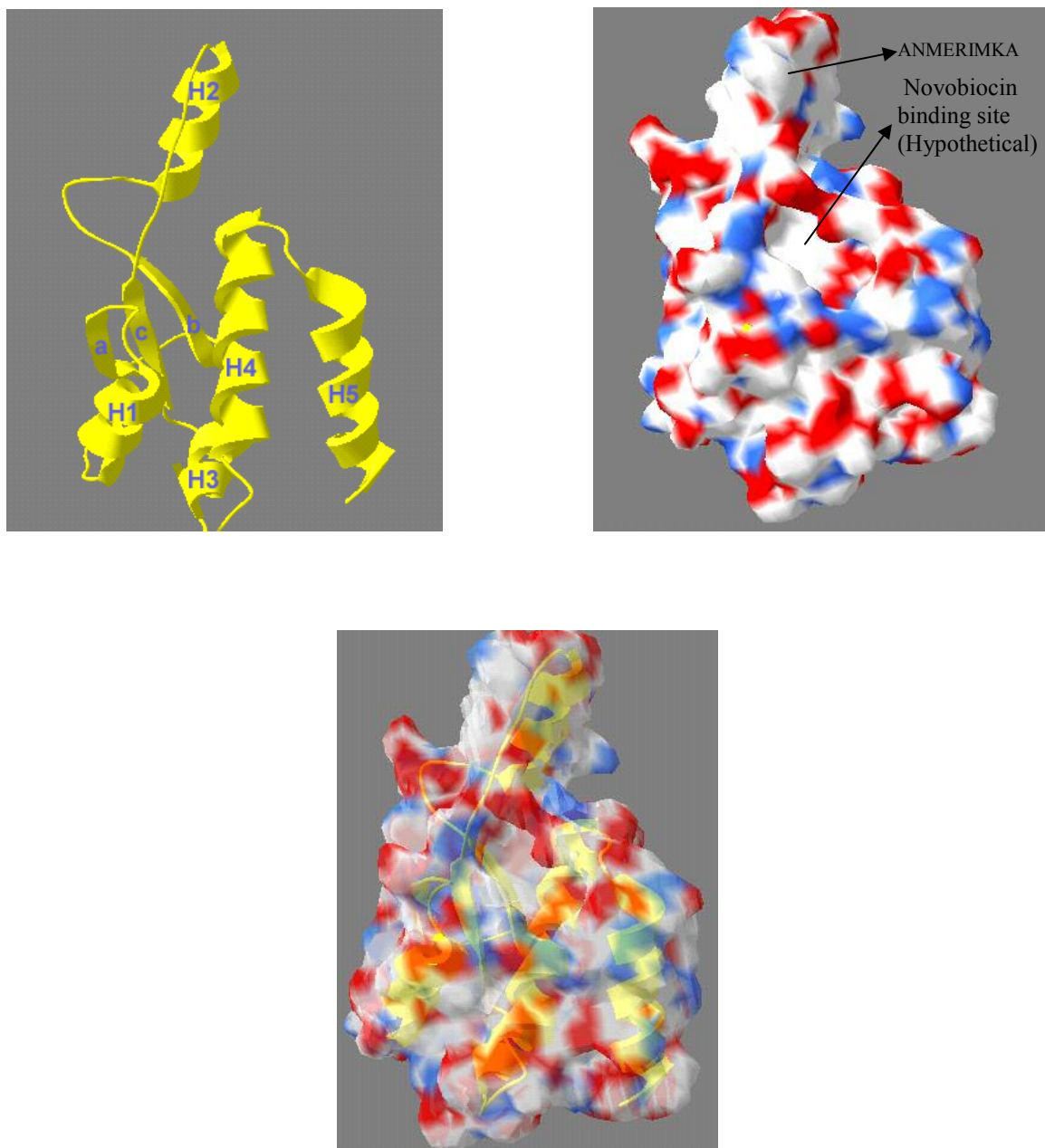


Figure 2: HtpG monomer structure (A) Helical structure of the HtpG monomer containing helices 4 and 5 that help in dimerization. B) Space fill model of the HtpG monomer, revealing a possible binding site for novobiocin. C) Overlapping model of HtpG containing both helical structures overlapped with spacefill model. ((Source: PDB, 1SF8, Model rendered by RASMOL)

Conformational states of Hsp90

Hsp90 has weak ATPase activity. Due to this weakness, the ATPase activity of Hsp90 remained controversial for some time. Reports from Wiech et al (36) suggested that purified Hsp90 failed to function as ATPase. In contrast, reports from Nadeau et al. (41) suggested that Hsp90 is an active ATPase. These inconsistencies were resolved following the crystallization of N-terminal domain of Hsp90 complexed with ADP (25). The ATP bound to Hsp90 is hydrolyzed making Hsp90 an ATPase. Hsp90 shared its structural homology with homodimeric ATPases such as gyrase, histidine kinase, Mut L. These proteins were called as GHKL superfamily. GHKL family is a strong model that guides most of the field's thoughts about Hsp90.

In this model, the N terminal domain binds to ATP through structure called as Bergerat fold (42, 43). Binding of ATP causes the dimerization of N terminal domain forming a “molecular clamp” (Figure 3, left). The dimerization of N terminal requires the pre dimerization of the C-terminal domain of Hsp90 (24). ATP hydrolysis results in the disruption of the C-terminal dimerization domain. This is a simple model for studying the Hsp90 mechanisms; however the mechanism underlying protein folding by Hsp90 is very complex and is still to be explored.

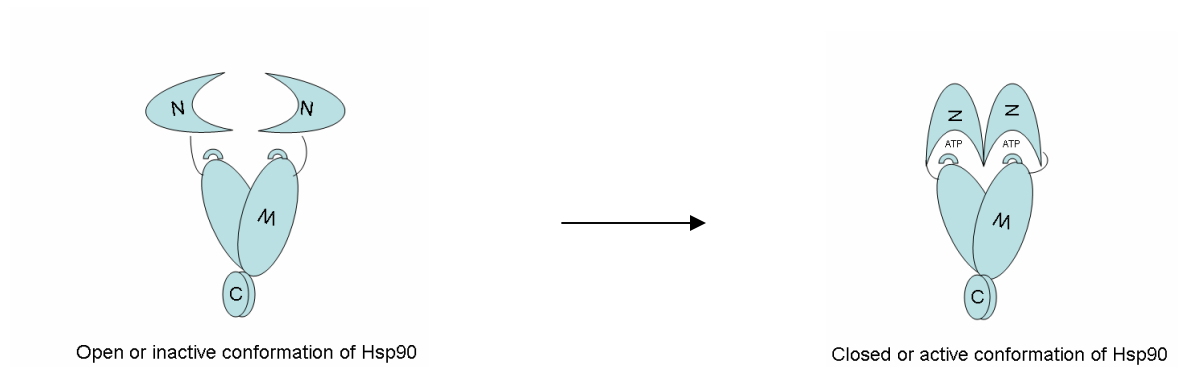


Figure 3: The open and closed conformation of Hsp90:

The open conformation of Hsp90, before the binding of ATP (Figure 3, left), binding of ATP induces the N- terminal domain to form lid segments which holds ATP. The ATP binding initiates an N- terminal dimerization (Figure 3, right). (Adapted and redrawn from **Prodromou** et al (31).

Geldanamycin and molybdate inhibit Hsp90's ATPase cycle

The molecular clamp model suggests that Hsp90 exists in two conformational states. The open and closed conformations are characterized by Hsp90's affinity for phenyl sepharose when bound to ADP and its affinity for p23, when ATP is bound (1, 27). The conformational changes of Hsp90 have been characterized by the effect of geldanamycin and molybdate. Geldanamycin binds to the N-terminal ATP binding site of Hsp90 (24, 28). Geldanamycin competes with nucleotides and locks Hsp90 in an open conformation (Figure 4A) and is found to mimick the ADP bound conformation of Hsp90, preventing the binding of ATP to Hsp90. In contrast to geldanamycin, molybdate locks Hsp90 in an ATP or ADP.Pi conformation that interacts tightly with substrates. However, molybdate induced conformational changes on Hsp90 require ATP (Figure 4B). The two different conformations induced by geldanamycin versus molybdate have characteristic proteolytic fingerprints (46, 47). Molybdate enforces a protease-resistant conformation at a major cleavage site present at Region 600 of human Hsp90 which contains an ANMERIMKA motif (47, 48, and 49). However, geldanamycin-bound Hsp90 fails to induce proteolytic-resistant conformation on the C-terminal domain of Hsp90.

Hsp90 ATPase cycle

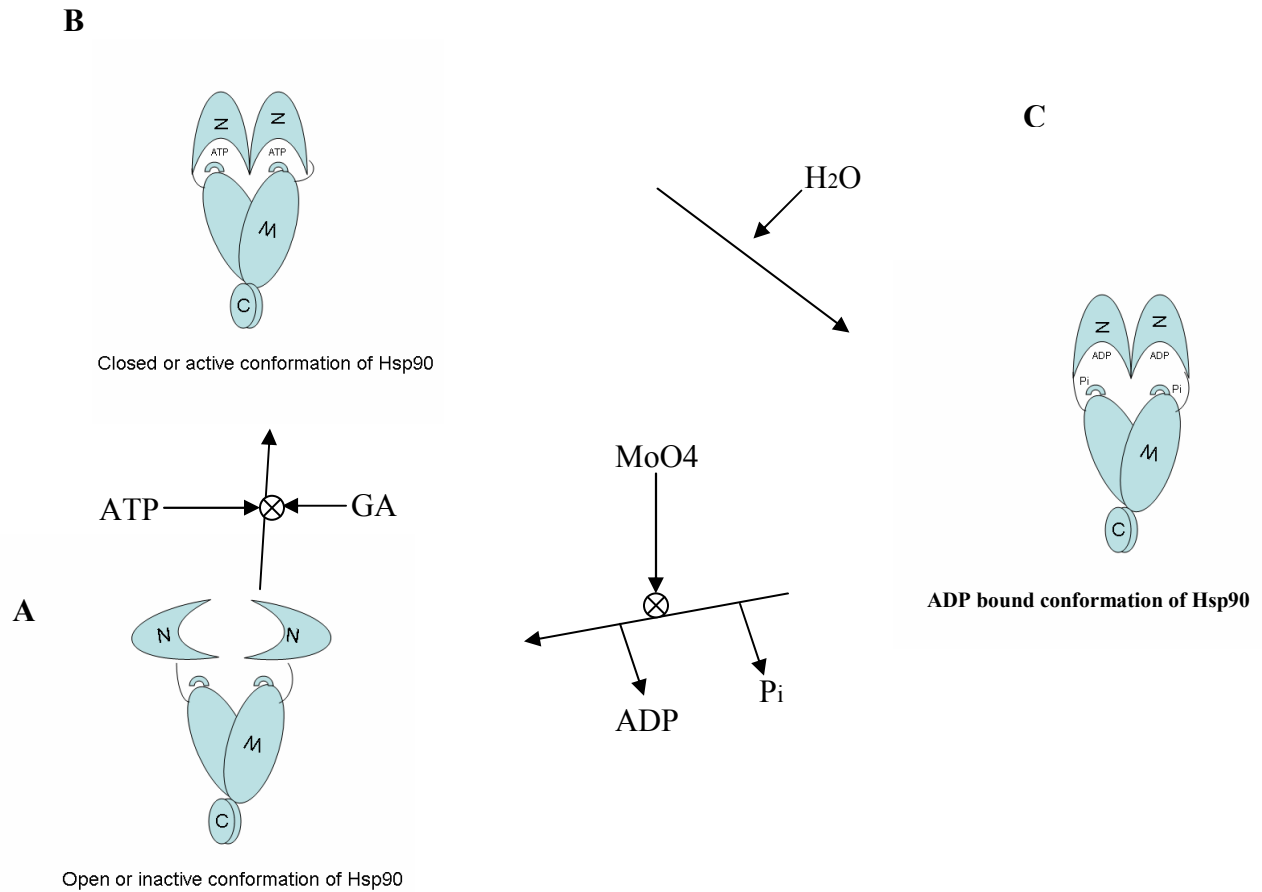
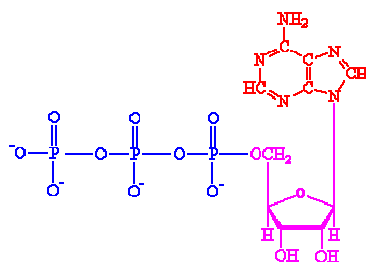


Figure 4: Model of ATPase cycle of Hsp90. (A) Hsp90 in its default conformation with its N terminal binding site empty. (B) Hsp90 containing ATP bound to the N terminal domain. (C) Hydrolysis of ATP bound to Hsp90 leading to formation of ADP and Pi.

Novobiocin inhibits Hsp90 function

Hsp90 shares structural homology with the ATP-binding domain of bacterial DNA gyrase B protein (24, 27, 43, 51 and 52). Coumarin antibiotics (novobiocin, chlorobiocin and coumermycin) were reported to bind to the nucleotide-binding site on Gyrase B. Since Hsp90 has a nucleotide-binding site similar to gyrase B protein, Neckers et al., analyzed the ability of novobiocin to inhibit chaperone function of Hsp90. They found that novobiocin treatment lead to the depletion Hsp90-dependent signal proteins (e.g., mutated p53, Raf-1, p60^{v-src} tumor cells) (53). Similarly, the Hsp90 dependent HRI kinase requires Hsp90 and Cdc37. However, novobiocin binding to Hsp90 causes the disruption of co-chaperone complex leading to the inhibition of the Hsp90 dependent activation/transformation of HRI (37). These results suggest the inhibition of Hsp90 function by novobiocin.

(A)



(B)

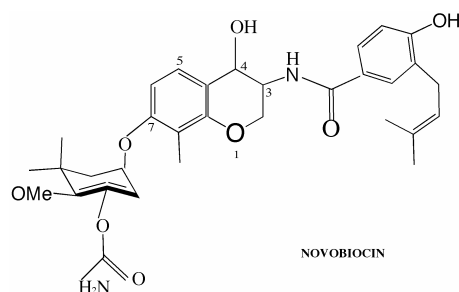


Figure 5: Structure of (a) ATP and (b) novobiocin

Other natural compounds may inhibit Hsp90

De novo folding of Lck into active form is mediated by Hsp90 *in vivo* and can be modeled in cell free reticulocyte lysates (RRL). Geldanamycin disrupts the interaction of Hsp90 interaction with Lck. Moreover, the Lck synthesized in the presence of geldanamycin was found to be functionally inactive (46).

Epigallocatechin gallate (Figure 6), a compound derived from green tea, has been recently reported to bind to Hsp90 leading to the inhibition of gene transcription of Aryl Hydrocarbon receptor gene (54). This prompted us to determine the effect of epigallocatechin gallate on the Hsp90 mediated folding of Lck.

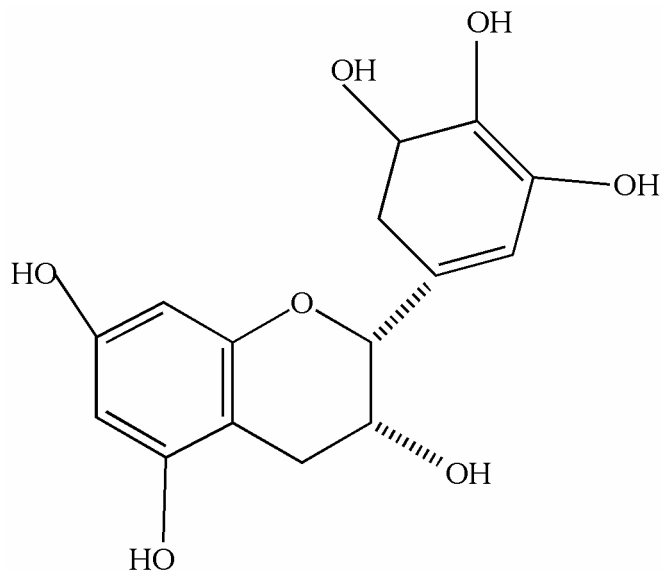


Figure 6: Structure of epigallocatechin gallate

The idea that curcumin (Figure 7) might bind and inhibit Hsp90 is very recent. Curcumin has been suggested to be an inhibitor of ATPase activity of Hsp90 (Dr.Matts personal communication). To investigate the ability curcumin, novobiocin and epigallocatechin gallate to inhibit Hsp90 mediated folding of client proteins; we used lymphoid cell kinase as a model substrate.

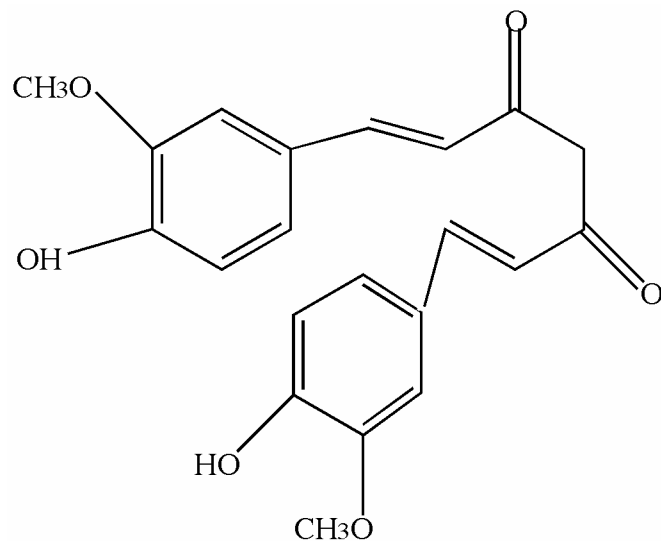


Figure 7: Structure of curcumin (adapted from sigma, redrawn using Chemdraw)

CHAPTER-II

MATERIALS AND METHODS

Reagents:

Novobiocin (M.W 634.61, Sigma (5N-6160) was dissolved in DMSO at 0.31 g/10 ml to make a 50 mM stock. Epigallocatechin gallate (M.W 458.4, Cayman chemical (70935) was dissolved in DMSO at 0.1 g/4.4 ml to make a 50 mM stock. Curcumin (M.W 368.38, Sigma C7727) was dissolved in DMSO at 0.36g /2 ml to make a 50 mM stock. Sodium molybdate (M.W 241.95, Sigma 331058) was dissolved in 2 ml of water to make a 100 mM stock. For each of these drugs, aliquots were stored at -20 °C and discarded after every use. Geldanamycin (M.W 560.6, obtained from Dr. Robert L Matts) was of 4µg/µl dissolved in DMSO and stored at -80 °C. Geldanamycin stocks were re-frozen after use. Rabbit reticulocytes were obtained from Promega. TPCK-treated Trypsin (Sigma 035K7676) was dissolved in trypsinolysis Buffer (10mM Tris HCl pH7.4, 150mM NaCl, 4mM CaCl₂, 0.1mM EDTA) at a concentration of 1µg/µl. Enolase (Sigma #112H9645) was prepared as previously described (Cooper et al (1984).

Hsp90 was detected with two antibodies namely, AC88 (a monoclonal antibody recognizing the C terminus of hsp90, was a gift from Dr. David Toft ,Mayo Medical School, Rochester, MN), and antibody PA 3-013 (Affinity Bioreagents, Inc.,) recognizing the N terminus of hsp90. Cdc37 was detected using polyclonal mouse anti-cdc37 antibodies (Hartson et al., (2000).

Immunoabsorption wash buffers:

Buffers contained 10mM PIPES and varied salt concentrations and detergents: 10 mM PIPES, 150 mM NaCl, 0.1% Tween pH7.0,(P150T), 10 mM PIPES, 500 mM NaCl, 0.1% Tween pH 7.0, (P500T), 10 mM PIPES pH 7.0, 50 mM NaCl pH7.0, (P50). Kinase wash Buffer contained (0.05M HEPES ,0.5% Triton X100, 0.1M NaCl, 1mM sodium ortho vanadate, pH7.4) and final Immunoprecipitation wash buffer contained (0.1M PIPES pH 7.0, 1.0M MnCl₂ , pH7.4).

Purification and protease finger printing of recombinant Hsp90:

Hsp90's C-terminal domain (Q531-D732), a PCR product of human Hsp90 encoding was ligated to pQE32 as previously described in (Yun et al., 2004). The C-terminal domain of Hsp90 was expressed in *E. coli* and purified to apparent homogeneity using HIS-SELECTTM Nickel affinity resin (Sigma P6611) as described (1). The protein was eluted from the resin using buffer containing 0.25M imidazole. After elution, fractions were analyzed by SDS-PAGE. Peak fractions were pooled and dialyzed against 10mM Tris HCl, 75mM NaCl (pH7.4). The dialyzed samples were aliquoted (~80 µg/40 µl), frozen with liquid nitrogen and stored at -80 °C. This protein was designated "Hsp90-CT"

For protease assays, 40µl of purified Hsp90-CT or the Activator of Hsp90 ATPase (Aha1) protein was thawed, diluted to a final concentration of 0.8 µg/ µl with 60 µl of 20 mM Tris HCl (pH 7.4) and mixed well. The diluted protein was divided equally between two tubes. Drug was added to one tube and an equal volume of drug vehicle to the other. The tubes were mixed well and incubated in ice for 30 minutes. After 30 minutes, aliquots of drug- treated Hsp90-CT and untreated Hsp90-CT were mixed 25µl of

assay buffer (10mM Tris HCl pH7.4, 150mM NaCl, 4mM CaCl₂, 0.1mM EDTA) containing indicated amounts of trypsin. The trypsinolysis reactions were incubated on ice for 6 minutes. The reactions were terminated by adding boiling SDS-PAGE sample buffer, and the samples were analyzed by SDS-PAGE.

Protease finger printing of Hsp90 in situ

Rabbit reticulocyte lysate containing an ATP regenerating system (10 mM creatine phosphate and 20units/ml creatine phosphokinase) were treated with drug or with drug vehicle control, and were incubated for 10 minutes at 30 °C. When a second drug was present, drugs were added to the reactions after the first incubation and the reactions were incubated further for 10 minutes at 30 °C. Drug-treated lysate were aliquoted into three tubes containing 150 µg/ ml of trypsin in 50 µl of assay buffer (10 mM Tris HCl pH7.4, 150 mM NaCl, 4 mM CaCl₂, 0.1 mM EDTA) and incubated on ice for 8 minutes. The reactions were terminated by adding the each reaction to boiling SDS-PAGE sample buffer, and the samples were analyzed by SDS-PAGE. The Hsp90 fragments containing the C terminus were detected by Western blotting with AC88 antibody.

Analysis of the effects of drugs on Hsp90 –substrate interactions:

Wild type lymphoid cell kinase (Lck) was used to determine the effect of novobiocin, epigallocatechin gallate, curcumin, geldanamycin on Hsp90s interactions with client protein kinase. In vitro transcription/translation reactions contained 9.6 µl of TnT Buffer (0.05 M creatine phosphate, 0.01 mM Magnesium acetate, 0.5 M potassium acetate, 0.1 mM amino acid-Met, 4 mM NTP's, pH7.30), 1 µl plasmid DNA (Lck wild type), 1 µl of [³⁵S] methionine, 35 µl of rabbit reticulocyte lysate (nuclease-treated) and 1 µl of SP6 RNA polymerase to a final volume of 50 µl. Control reactions lacked plasmid

and SP6 polymerase. Drugs were immediately added to the individual tubes and mixed well. The [35 S]Lck was synthesized for 45 minutes at 30 °C by coupled transcription/translation (TnT). Incorporation of [35 S] met was determined by TCA protein assay or by autoradiography. Since novobiocin was found to inhibit the TnT reaction, novobiocin was added 25 minutes after initiation of transcription and translation. After 45 minutes of incubation, 45 μ l of reaction was used for co-immunoprecipitation. Control reactions testing the for the direct inhibition of Lck by drugs, drugs were added at the beginning and 80 minutes after initiation of transcription and translation.

Kinase activity of Lck:

Protein A resin (Sigma) was used to bind α -Lck antibody by rocking at 4 °C for 1.5 hours. The tubes were then washed once with P150T, once with P500, twice with P50 wash buffers. After the final wash, the tubes were centrifuged again and the supernatant was aspirated using a 20 μ l pipette. The immunopellets was then mixed with lysate (45 μ l) in presence of 250 μ l of final immunoprecipitation wash buffers, and rocked for 2 hours at 4 °C. Immunoabsorbed mixtures were washed once with Kinase wash buffer, followed by two washes with final immunoprecipitation wash buffers. After the final wash, the tubes were centrifuged again, and the remaining supernatant was aspirated off.

Immediately before use, 10 μ l (44 μ g) of enolase was mixed with 10 μ l of enolase denaturation buffer (50 mM sodium acetate /acetic acid pH 3.3). The tubes were gently mixed and incubated at 30 °C for 5 minutes. The tubes were then held on ice until further use. Kinase Assay Mix (KAM) containing 0.5M PIPES pH 7-7.2, 0.1M MnCl₂, 22 μ g

acid denatured enolase, 0.1 mM ATP stock, ^{32}P ATP (40 μCi or 100 μCi) was prepared immediately before adding to the immunopellet. KAM was aliquoted (25 μl) equally to individual reaction tubes and mixed well for 15 minutes at 30°C. The reactions were terminated by boiling in SDS-PAGE sample buffer and analyzed by SDS-PAGE gel and western blotting. [^{32}P]Lck and [^{32}P]enolase were detected by autoradiography and densitometry.

CHAPTER-III

RESULTS

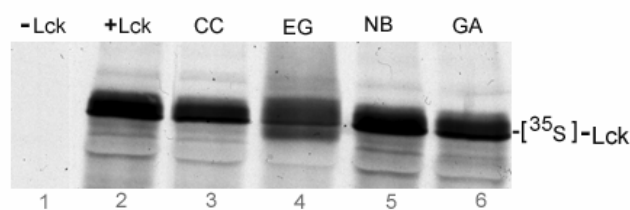
Curcumin, epigallocatechin gallate and novobiocin inhibit Hsp90-dependent folding of Lck:

To characterize the effect of curcumin, epigallocatechin gallate and novobiocin on Hsp90-mediated chaperone function, Lck was used as Hsp90 model substrate. Hsp90 has been shown to mediate the proper folding and functioning of Lck (46). For these assays, Lck was synthesized and matured in the presence of curcumin, novobiocin, epigallocatechin gallate and geldanamycin was immunoadsorbed. The drugs curcumin, novobiocin and geldanamycin did not inhibit the efficiency of synthesis of Lck (Figure 8A, lane 3, 5, 6). However, epigallocatechin gallate inhibited Lck synthesis, thus epigallocatechin gallate was added 20 minutes after the on-set of transcription and translation. Matured Lck had a different electrophoretic mobility when treated with epigallocatechin gallate (Figure 8A, lane 4).

After immunoadsorption, Lck was assayed with [32 P]ATP for its phosphotransferase activity. Lysates treated with had a kinase activity of 1% (Figure 7A, lane 6) when compared to drug control (DMSO) (Figure 8B, lane 2). Lysates treated with curucmin also produced Lck molecules deficient in kinase activity (67 %) (Figure 8B, lane 3). Lysates treated with novobiocin produced Lck deficient in kinase activity (17%) (Figure 8B, lane 4). Similarly, Lck molecules synthesized in presence of epigallocatechin gallate displayed decreased phosphotransferase activity (33%) (Figure

8B, lane 4). These results showed that these drugs lead to the production of Lck molecules deficient in their phosphotransferase activity.

A



B

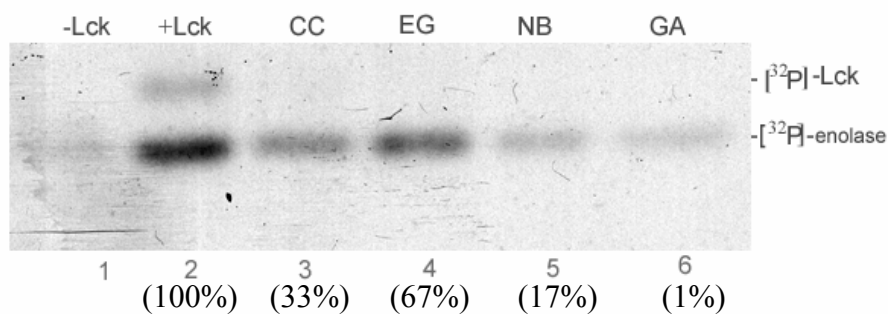


Figure 8: Effect of curcumin, epigallocatechin gallate, novobiocin and geldanamycin on Hsp90-mediated folding of Lck. Lck was synthesized in reticulocyte lysate reactions containing $[^{35}\text{S}]$ -met and curcumin, novobiocin, and geldanamycin or drug vehicle. Epigallocatechin gallate was added to lysate 20 minutes after the onset of transcription and translation and lysates were incubated for further 25 minutes. Lck was isolated by immunoadsorption, incubated with $[^{32}\text{P}]$ ATP and analyzed by SDS-PAGE and autoradiography. Metabolically labeled and kinase assay products are indicated in Panel A, Panel B respectively. Under Panel B: numbers represent the densitometry quantitation acquired from autoradiogram.

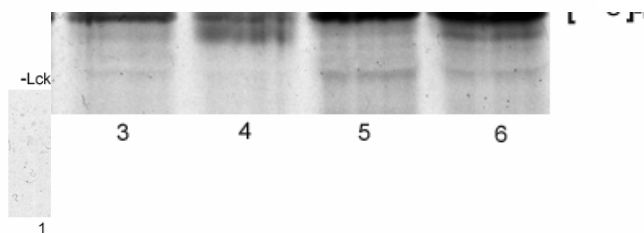
Curcumin, epigallocatechin gallate and novobiocin do not inhibit Lck directly

To determine whether curcumin, epigallocatechin gallate and novobiocin inhibited Hsp90-mediated folding of Lck versus inhibiting the Lck directly, Lck was synthesized and matured in rabbit reticulocyte for 80 minutes in absence of drugs. After synthesis and maturation, drugs were added to the lysate, and reactions were chilled on ice for 3 minutes on ice. Lck was immunoadsorbed and incubated with [³²P]ATP to determine its phosphotransferase activity. Autoradiography analysis of the immunoadsorbed Lck suggested that curcumin-, novobiocin- and geldanamycin-treated lysate exhibited a uniform Lck kinase activity, suggesting that these drugs do not inhibit kinase directly under these assay conditions (Figure 9B, lower band).

Epigallocatechin gallate induced altered electrophoretic mobility on Lck. This suggests that epigallocatechin gallate mediates change in the structure of Lck (Figure 9A, lane 4). Epigallocatechin gallate treated Lck, showed slightly decreased kinase activity (15 %), probably due to the structural modifications induced by epigallocatechin gallate (Figure 9B, Lane 4). Epigallocatechin gallate added to Lysate containing immature Lck displayed decreased kinase activity (67%). Similarly, epigallocatechin gallate added to Lysate containing mature Lck displayed decreased kinase activity (70%), suggesting that the decrease in kinase activity of Lck (Figure 9B, lane 4) could not be attributed to epigallocatechin gallate

These results suggest that curcumin, novobiocin and some of epigallocatechin gallate do not inhibit Lck directly under these assay conditions.

A



B

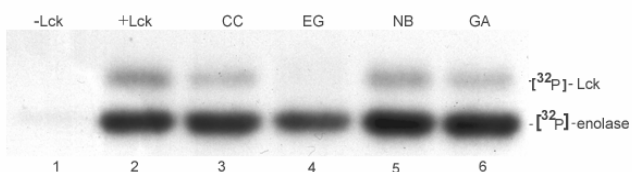


Figure 9: Curcumin, epigallocatechin gallate and novobiocin do not inhibit kinase directly. Lck was synthesized in reticulocyte lysate reactions for 80 minutes. After 80 minutes lysates were treated curcumin, epigallocatechin gallate, novobiocin, geldanamycin (or) DMSO. Lysates were then chilled in ice for 3 minutes. Lck was isolated by immunoadsorption and Lck kinase activity was analyzed by using $[^{32}\text{P}]\text{ATP}$ and analyzed by SDS-PAGE and autoradiography. Metabolically labeled and kinase assay products are indicated in Panel A, Panel B respectively.

Effect of curcumin, epigallocatechin gallate and novobiocin on interaction of Lck and Hsp90

To test the hypothesis that curcumin, epigallocatechin gallate and novobiocin disrupted the interaction of Lck with Hsp90, Lck was immunoadsorbed and the interaction of Lck with Hsp90 and its co-chaperone Cdc37 was assayed by Western blotting. The drug vehicle (DMSO) did not disrupt the interaction of Lck with its Cdc37 and Hsp90 chaperones (Figure 10B, lane 2). In contrast, geldanamycin completely disrupted the Lck interaction with Hsp90, consistent with the previous reports (46). Novobiocin (5 mM) disrupted the Lck interaction with Hsp90 (Figure 10B, Lane 5).

The new candidate epigallocatechin gallate, however did not disrupt the interaction of Lck with Hsp90 and Cdc37 completely (80%, 64% respectively) (Figure 10B, lane 4). Similarly, curcumin did not disrupt the interaction of Lck with Hsp90 and Cdc37 completely (80%, 90% respectively) (Figure 10B, lane 3). These results suggest that the novobiocin and geldanamycin disrupts Hsp90 function by inhibiting the Lck interaction with Hsp90 and Cdc37 (100%). However, epigallocatechin gallate and curcumin inhibit Hsp90 function (33%, 67% respectively) without disrupting the interaction of Lck with Hsp90 and Cdc37 completely. (Figure 10B, lane 4). However, curcumin and epigallocatechin gallate are quantitatively less efficient in disrupting the interaction of Hsp90 and Cdc37 with Lck compared to novobiocin and geldanamycin.

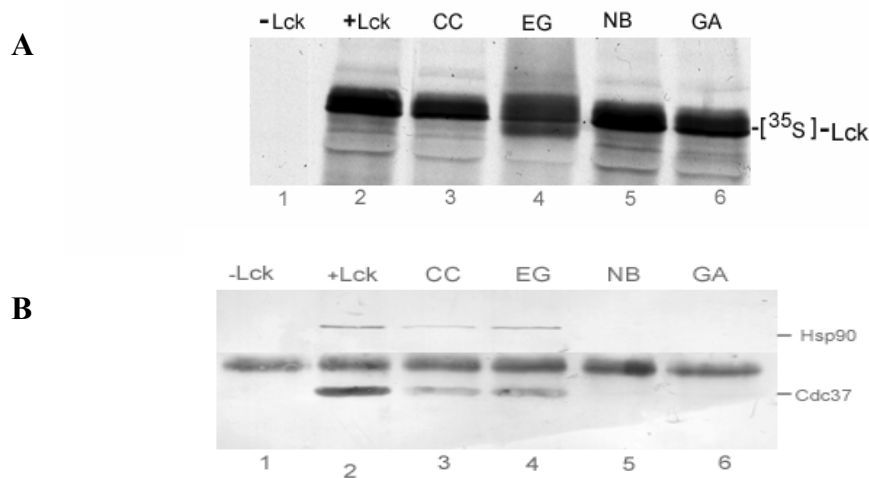
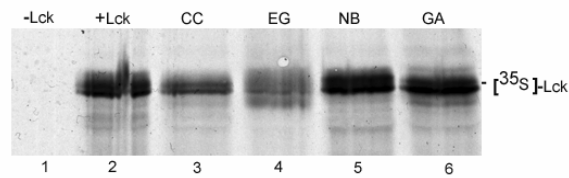


Figure 10: Effect of curcumin, epigallocatechin gallate and novobiocin on interaction of Lck and Hsp90 in RRL. Lck was synthesized and matured in reticulocyte lysates translation reactions containing curcumin, novobiocin and geldanamycin or drug vehicle (DMSO). Epigallocatechin gallate was added to lysate 20 minutes after the onset of transcription and translation and lysates were incubated for further 25 minutes. After incubation, Lck was isolated by immunoadsorption and Lck interaction with its co-chaperones Hsp90 and Cdc37 was analyzed by SDS-PAGE and Western blotting with anti-rabbit Hsp90 and anti-mouse Cdc37. Metabolically labeled and Western blot of Lck interaction with Hsp90 and Cdc37 are presented in Panel A, Panel B respectively.

Effect of curcumin, epigallocatechin gallate and novobiocin on the interaction of *mature* Lck with Hsp90

To test the hypothesis that of maturation Lck would be independent of Hsp90 machinery, mature Lck was immunoadsorbed after 80 minutes in RRL and assayed by Western blot. The drug vehicle (DMSO) did not disrupt the interaction of Lck with its Cdc37 and Hsp90 chaperones (Figure 11B, lane 2). Geldanamycin has been reported to disrupt the interaction of Hsp90 with its co-chaperones strongly (46). In contrast, I find that geldanamycin does not disrupt the interaction between Hsp90, mature Lck and Cdc37, suggesting that the data is not interpretable. Together these results suggest that the ability of these drugs to inhibit Hsp90 is not related with this association of Hsp90 with its co-chaperones.

A



B

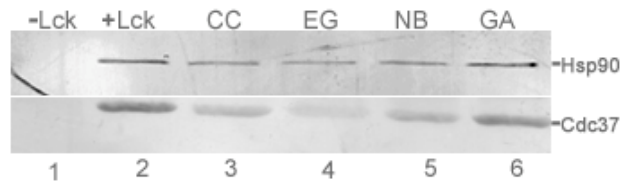


Figure 11: Curcumin, epigallocatechin gallate and novobiocin do not inhibit kinase directly: Lck was synthesized in reticulocyte lysate reactions for 80 minutes. After 80 minutes lysates were treated curcumin, epigallocatechin gallate, novobiocin, geldanamycin (or) DMSO. Lysates were then chilled in ice for 3 minutes. Lck was isolated by immunoadsorption and Lck interaction with its co-chaperones Hsp90 and Cdc37 was analyzed by SDS-PAGE and Western blotting with anti-rabbit Hsp90 and anti-mouse Cdc37. Metabolically labeled and Western blot of Lck interaction with Hsp90 and Cdc37 are presented in Panel A, Panel B respectively.

Molybdate and geldanamycin have opposite effects on Hsp90

Drug-induced conformational changes on Hsp90 can be analyzed by proteolytic nicking assays. Hartson et al. (46), Yun et al. (38) suggest that in rabbit reticulocyte lysate treated with 20 mM molybdate, Hsp90 assumes a protease-resistant conformation. However, geldanamycin prevents molybdate-induced conformational changes on Hsp90.

To benchmark previous observations and to determine the effects of molybdate and geldanamycin on the conformation of Hsp90, rabbit reticulocyte was treated with 17 μ M geldanamycin or 5 mM molybdate, and their effects on structural conformation of Hsp90 was assayed by trypsinolysis. Molybdate induced protease-resistant conformation on Hsp90 (Figure 12, lane 3). Geldanamycin was unable to enforce protease-resistant conformation on Hsp90 (Figure 12, lane 2), an observation consistent with previous observations by (46).

Grenert et al. (27) report that geldanamycin and ATP compete for same binding site on Hsp90. Molybdate's inability to induce a protease-resistant conformation on Hsp90 in lysate treated with geldanamycin (Figure 12, lane 4) demonstrates that the molybdate induced protease-resistant conformation of Hsp90 requires ATP to be bound to Hsp90,

Roe et al. (28) indicate that K_d of geldanamycin for Hsp90 is 1.2 μ M. However, molybdate (20 mM) induced protease-resistant conformation on Hsp90 cannot be reversed even in the presence of 17 μ M geldanamycin (Figure 12, lane 5), suggesting that even very high concentrations of geldanamycin cannot displace bound ATP from Hsp90 in presence of molybdate. However, In the presence of low concentrations of molybdate (5 mM), geldanamycin reverses the molybdate-induced conformational changes on the C-

terminal domain of full-length Hsp90. These results suggest that molybdate induced proteolytic-resistant on Hsp90 is concentration dependent.

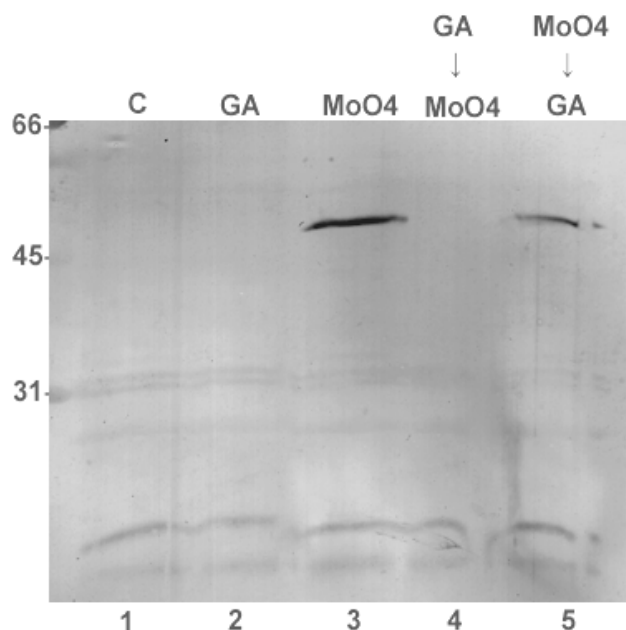


Figure 12: Effect of molybdate and geldanamycin on structural conformation of Hsp90. Lysates containing ATP-regenerating system were treated with molybdate (5 mM) and geldanamycin (17 μ M) and incubated at 30 °C for 10 minutes. Additional drugs were added and lysate was incubated for further 10 minutes at 30 °C (MoO₄ \rightarrow GA, GA \rightarrow MoO₄). Lysates were then trypsinolyzed for 8 minutes at 4 °C. Reactions were terminated by the addition of boiling SDS-PAGE buffers. Proteins were analyzed by SDS-PAGE and Western blotting with antibodies directed against C- terminus of Hsp90.

Effect of novobiocin on the conformation of Hsp90 (rabbit reticulocyte lysate)

To test the hypothesis that novobiocin inhibited Hsp90 by a molybdate-like mechanism, novobiocin and or molybdate were added to rabbit reticulocyte lysate and their impact on Hsp90 conformation was compared. As observed previously, 5 mM molybdate was able to enforce a conformational change on Hsp90, producing a conformational change on the C-terminal domain of Hsp90 (Figure 13, lane 2). Novobiocin failed to enforce proteolytic-resistant conformation on Hsp90 (Figure 12, lane 4), suggesting that novobiocin has a mechanism of action different from molybdate.

However, a previous report by Yun et al. (38) suggests that in lysates treated with 20 mM molybdate and 0-5 mM novobiocin, novobiocin potentiates molybdate's ability to enforce a conformational change on Hsp90. However, in lysates treated with 5 mM molybdate and 5 mM novobiocin, novobiocin could not potentiate the molybdate effect (Figure 13, lane 5). Moreover, novobiocin reverses the molybdate induced conformational changes on the C-terminal domain of Hsp90. These results suggest that novobiocin fails to potentiate molybdate's ability to induce proteolytic- resistant conformation on Hsp90, suggesting the hypothesis that novobiocin inhibited Hsp90 by a molybdate-like mechanism is false.

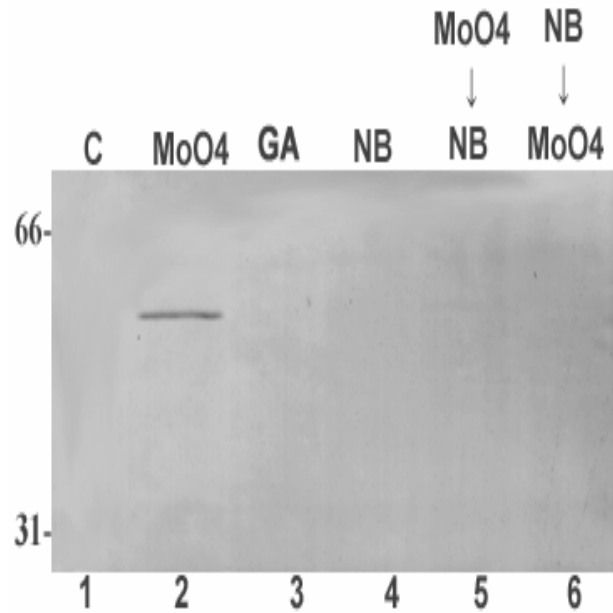


Figure 13: Effect of novobiocin on structural conformation of Hsp90. Lysates containing ATP-regenerating system were treated with novobiocin (5 mM), molybdate (5 mM) or geldanamycin (17 μ M) and incubated at 30 °C for 10 minutes. Additional drugs were added and incubated for further 10 minutes at 30 °C (MoO₄ \rightarrow NB, NB \rightarrow MoO₄). Lysates were then trypsinolyzed for 8 minutes at 4 °C. Reactions were terminated by the addition of boiling SDS-PAGE buffers. Proteins were analyzed by SDS-PAGE and Western blotting with antibodies directed against C- terminus of Hsp90.

Novobiocin reverses molybdate induced conformational changes on the C-terminal domain of full length Hsp90

To benchmark previous observations and to determine the effects of molybdate and novobiocin on the conformation of Hsp90, rabbit reticulocyte lysates were treated with 20 mM molybdate with an increasing concentration of novobiocin (0-7.5 mM). Molybdate induced proteolytic-resistant conformation on Hsp90 (Figure 14, lane 2). Increasing concentrations of novobiocin potentiated the molybdate- induced conformational changes on C-terminal domain of Hsp90 up to 0-2 mM (Figure 14, lane 3-5). At a concentrations greater than 5 mM, novobiocin reversed the molybdate- induced conformational changes on the C-terminal domain of Hsp90. Novobiocin's ability to completely reverse the molybdate induced conformational change on Hsp90 is evident at novobiocin concentration (7.5 mM). These results suggested that novobiocin's ability to potentiate molybdate-induced conformational changes and the ability of novobiocin to reverse the effect varied with novobiocin concentration.

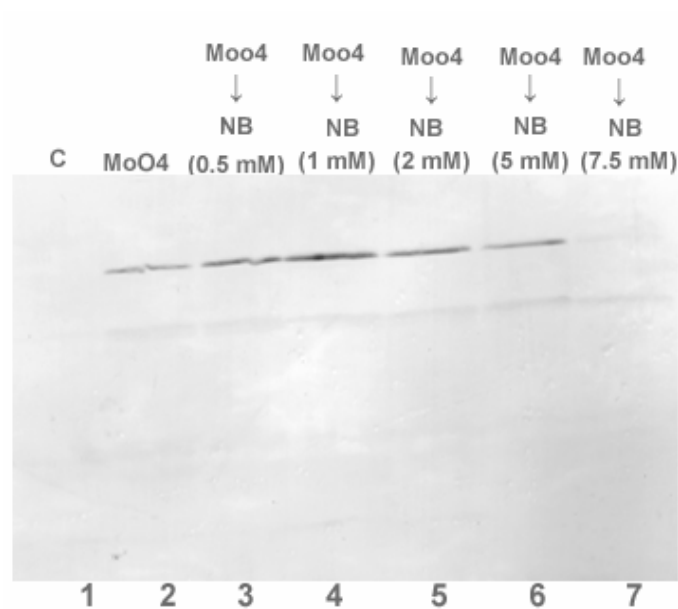


Figure 14: Novobiocin reverses molybdate induced conformational changes on the C-terminal domain of full length Hsp90. Lysates containing ATP-regenerating system were treated with molybdate (20 mM) and incubated at 30 °C for 10 minutes. Additional drugs were added and lysate was incubated for further 10 minutes at 30 °C (Moo4 →NB). Lysates were then trypsinolyzed for 8 minutes at 4 °C. Reactions were terminated by the addition of boiling SDS-PAGE buffers. Proteins were analyzed by SDS-PAGE and Western blotting with antibodies directed against C-terminus of Hsp90.

Effect of epigallocatechin gallate on the conformation of Hsp90 (rabbit reticulocyte lysate)

Epigallocatechin gallate has been recently reported to inhibit transcription of aryl hydrocarbon receptor indirectly by binding to Hsp90 (54). To investigate the effect of epigallocatechin gallate on the conformation of Hsp90 and also to test the hypothesis that epigallocatechin gallate inhibited Hsp90 by a molybdate-like mechanism, 2 mM epigallocatechin gallate was added to the lysate and its impact on Hsp90 conformation was assayed by trypsinolysis. As seen previously, molybdate was able to enforce a protease-resistant conformation on Hsp90 (Figure 15, lane 2). Epigallocatechin gallate was unable to enforce a proteolytic-resistant conformation on Hsp90 (Figure 15, lane 3), suggesting epigallocatechin gallate has a mechanism different from molybdate. When molybdate was added to epigallocatechin gallate-treated lysate, epigallocatechin gallate did not enhance molybdate from inducing a proteolytic-resistant conformation on Hsp90 (figure 15, lane 5).

Previous reports by Hartson et al. (47) suggest that geldanamycin was unable to reverse 20 mM molybdate's ability to restructure Hsp90. However, epigallocatechin gallate was able to reverse the protease-resistant conformation induced by molybdate strongly (Figure 15, lane 4).

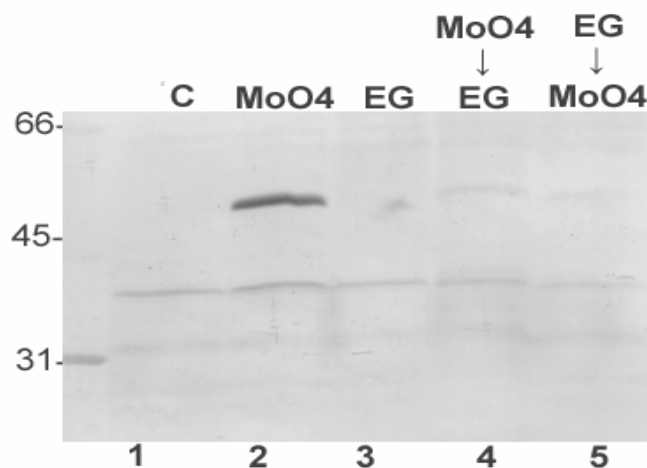


Figure 15: Effect of epigallocatechin gallate on Hsp90 conformation: Lysates containing ATP-regenerating system were treated with epigallocatechin gallate (2 mM), molybdate (5mM) and incubated at 30 °C for 10 minutes. Additional drugs were added and incubated for further 10 minutes at 30 °C (MoO4 → EG, EG → MoO4). Lysates were trypsinolyzed for 8 minutes at 4°C. Reactions were terminated by the addition of boiling SDS-PAGE buffers. Proteins were analyzed by SDS-PAGE and Western blotting with antibodies directed against C-terminus of Hsp90.

Effect of curcumin on the conformation of Hsp90 (rabbit reticulocyte lysate)

Curcumin has been recently suggested to inhibit the ATPase activity of Hsp90 (personal communication Dr. Robert L Matts). To investigate the effect of curcumin on the conformation of Hsp90 and to test the hypothesis that curcumin inhibited Hsp90 by a molybdate-like mechanism, 1 mM curcumin was applied to lysate and its impact on Hsp90 conformation was assayed by trypsinolysis. As observed previously, molybdate was able to enforce a conformational change on Hsp90 (Figure 16, lane 2). However, curcumin was unable to enforce a proteolytic-resistant conformation on Hsp90 (Figure 16, lane 4).

To check the hypothesis that curcumin was able to potentiate molybdate-induced change in Hsp90 conformation, lysates were treated with curcumin, followed by molybdate. Curcumin was unable to strengthen molybdate-induced conformational changes on Hsp90 (Figure 16, lane 3), suggesting that curcumin cannot potentiate molybdate effect. Additionally, curcumin was unable to prevent molybdate from enforcing a structural conformation on Hsp90 (Figure 16, lane 3). These results suggest that curcumin has a different effect on Hsp90, compared to geldanamycin and novobiocin.

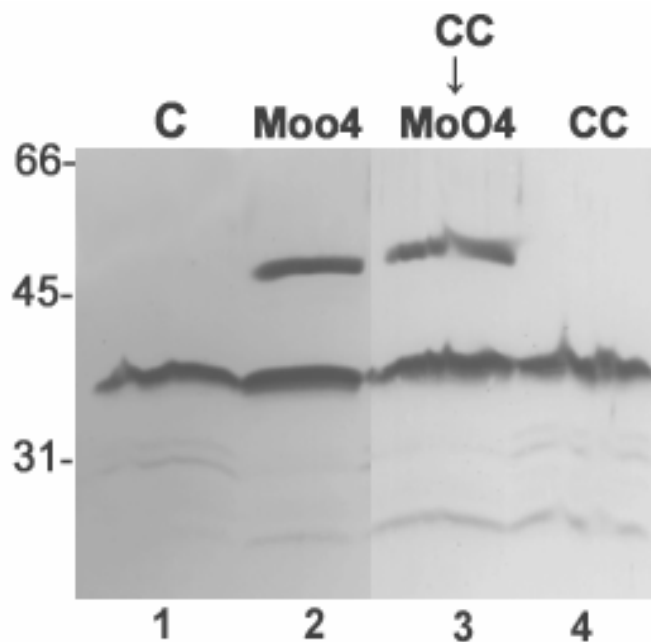


Figure 16: Curcumin has unique mechanism of action on Hsp90. Lysates containing ATP- regenerating system were treated with curcumin (1 mM) or molybdate (5 mM) and incubated for 10 minutes. Additional drugs were added and lysates were incubated for further 10 minutes at 30 °C (CC → MoO4) . Lysates were trypsinolyzed for 8 minutes at 4°C. Reactions were terminated by the addition of boiling SDS-PAGE buffers. Proteins were analyzed by SDS-PAGE and Western blotting with antibodies directed against C-terminus of Hsp90.

Curcumin and geldanamycin do not compete for same binding site on Hsp90

Curcumin has been recently suggested to inhibit the ATPase activity of Hsp90 (personal communication Dr. Robert I Matts). Curcumin's inability to prevent molybdate from enforcing proteolytic-resistant conformation on Hsp90 (Figure 17, lane 3), suggests that curcumin and geldanamycin do not share the same binding site on Hsp90. To test this hypothesis, lysates were incubated with 1 mM curcumin, 17 μ M geldanamycin and 5 mM molybdate and their impact on Hsp90 conformation was assayed by trypsinolysis. As observed previously, molybdate was able to induce proteolytic-resistant conformation on Hsp90 (Figure 17, lane 2). Curcumin was unable to prevent molybdate from enforcing a proteolytic-resistant conformation on Hsp90 (Figure 16, lane 5). Geldanamycin prevents molybdate from structuring Hsp90 (Figure 17, lane 3). Curcumin's did not prevent geldanamycin from having this effect (Figure 17, lane 4). Thus, curcumin and geldanamycin did not compete for same binding site on Hsp90 under these assay conditions.

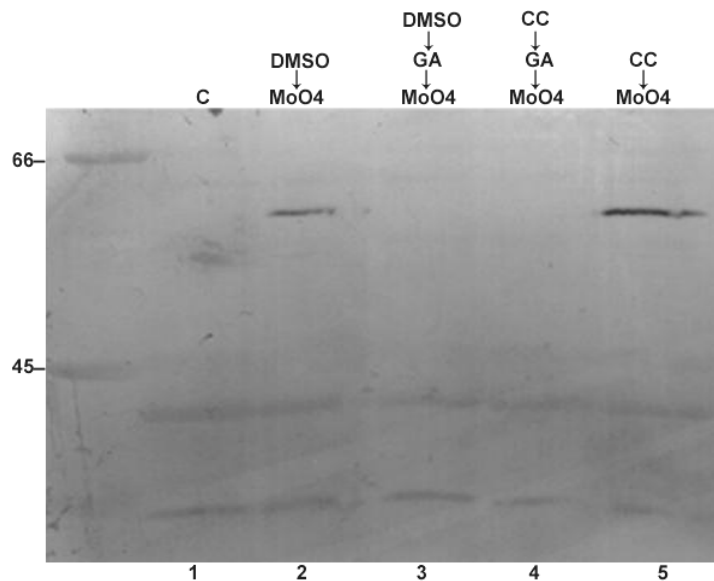


Figure 17: curcumin and geldanamycin do not compete for same binding site on Hsp90. Lysates containing ATP-regeneration system were treated with molybdate (5 mM), curcumin (1 mM) and geldanamycin (17 μ M) and incubated at 30 °C for 10 minutes. Additional drugs were added and incubated for further 10 minutes at 30 °C (DMSO→MoO₄, DMSO→GA→MoO₄, CC →GA→MoO₄, CC→MoO₄). Lysates were trypsinolyzed for 8 minutes at 4 °C. Reactions were terminated by the addition of boiling SDS-PAGE buffers. Proteins were analyzed by SDS-PAGE and Western blotting with antibodies recognizing the C-terminus of Hsp90.

Curcumin and epigallocatechin gallate do not compete for same binding site on Hsp90

To test the hypothesis that curcumin and epigallocatechin gallate share the same binding site on Hsp90, lysates were incubated with 1 mM curcumin, 2 mM epigallocatechin gallate and 5 mM molybdate. As observed previously, molybdate was able to induce a proteolytic-resistant conformation on Hsp90 (Figure 18, lane 2). Curcumin was unable to reverse the molybdate-induced proteolytic-resistant conformation of Hsp90 (Figure 18, lane 3). In contrast, epigallocatechin gallate was able to reverse the molybdate-induced conformation of Hsp90 (Figure 18, lane 4). Curcumin did not inhibit epigallocatechin gallate's ability to reverse molybdate effect (Figure 18, lane 5), suggest that epigallocatechin gallate and curcumin do not compete for binding under these assay conditions.

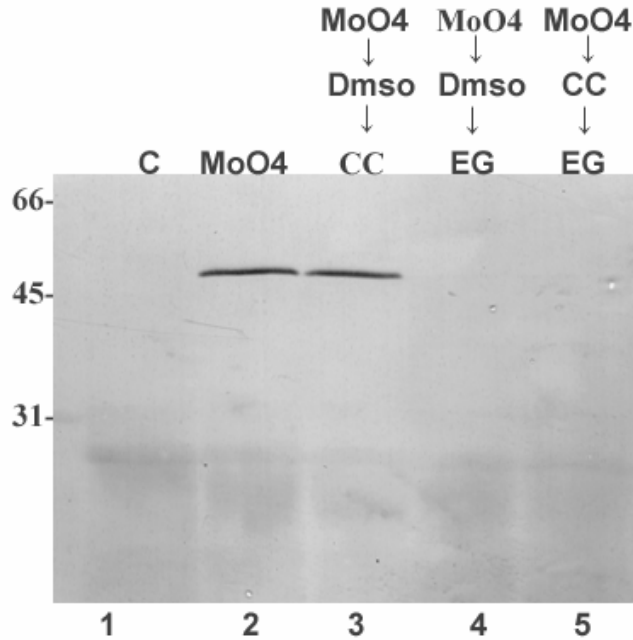


Figure 18: Curcumin and epigallocatechin gallate do not compete for same binding site on Hsp90. Lysates containing ATP- regenerating system were treated with curcumin (1 mM), molybdate (5 mM), epigallocatechin gallate (2 mM) and incubated at 30 °C for 10 minutes. Additional drugs were added and incubated for further 10 minutes at 30 °C (MoO4→ DMSO→CC, MoO4→ DMSO→EG, and MoO4→ CC→EG). Lysates were trypsinolyzed for 8 minutes at 4 °C. Proteins were analyzed by SDS-PAGE and Western blotting with antibodies recognizing the C-terminus of Hsp90.

Curcumin and novobiocin do not compete for same binding site on Hsp90

To test the hypothesis that novobiocin and curcumin do not bind to same binding site on Hsp90, lysates were incubated with 1 mM curcumin, 5 mM novobiocin and 5 mM molybdate. As previously described molybdate was able to enforce a proteolytic-resistant conformation on Hsp90 (Figure 19, lane 2). Curcumin was unable to prevent molybdate from enforcing a proteolytic-resistant conformation on Hsp90 (Figure 19, lane 3). As described previously, novobiocin was able to reverse molybdate- induced conformational changes on Hsp90 (Figure 19, lane 4). Curcumin was unable to prevent novobiocin's ability to reverse molybdate- induced conformational changes on Hsp90 (Figure 19, lane 5). This suggests that curcumin and novobiocin do not compete for the same binding site on Hsp90 under these assay conditions.

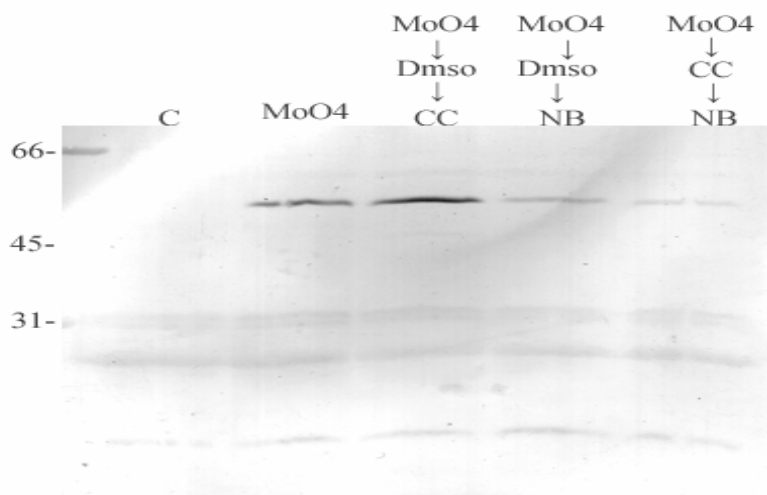


Figure 19: Curcumin and novobiocin do not compete for same binding site on

Hsp90. Lysates containing ATP- regenerating system were treated with curcumin (1 mM), molybdate (5 mM), novobiocin (5 mM) and incubated at 30 °C for 10 minutes. Additional drugs were added and incubated for further 10 minutes at 30 °C (MoO4→ DMSO→CC, MoO4→ DMSO→NB and MoO4→ CC→NB). Lysates were trypsinolyzed and incubated for 8 minutes at 4 °C. Proteins were analyzed by SDS-PAGE and Western blotting with antibodies recognizing the C-terminus of Hsp90.

Novobiocin, curcumin, epigallocatechin gallate do not inhibit trypsin

Drug-induced conformational changes on Hsp90 were analyzed by protease nicking assays. To test the hypothesis that the drugs novobiocin, curcumin and epigallocatechin gallate do not inhibit trypsin directly, the protein Activator of the Hsp90 ATPase (Aha1) was used as a proteolytic substrate. Aha1 was incubated with drug vehicle, novobiocin, curcumin, epigallocatechin gallate and trypsinolysed.

Aha1 was equally susceptible to trypsinolysis in the absence of drugs (Figure 20, lane 5) and in the presence of novobiocin (Figure 20, lane 2), curcumin (Figure 20, lane 3), epigallocatechin gallate (Figure 20, lane 4) suggesting that curcumin, epigallocatechin gallate and novobiocin do not inhibit trypsin.

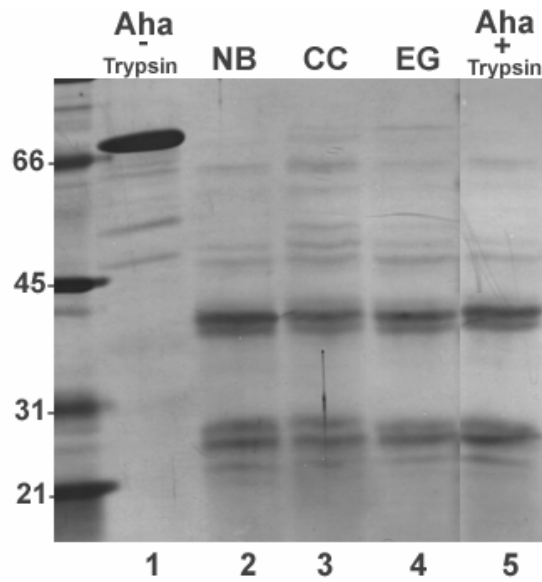


Figure 20: Novobiocin, curcumin, epigallocatechin gallate, do not inhibit trypsin.

Activators of Hsp90 ATPase (Aha1) was incubated with novobiocin (5 mM), curcumin (5 mM), epigallocatechin gallate (5 mM) for 30 minutes on ice. The reactions were trypsinolyzed and incubated for 6 minutes at 4 °C and analyzed by SDS-PAGE.

Novobiocin protects carboxy terminus of Hsp90 from cleavage by trypsin

Yun et al. (38) reported that novobiocin induces the purified truncated Hsp90 C-terminal domain of Hsp90 (Hsp90-CT, amino acid 584-730) to assume a protease-resistant conformation *invitro*.

To confirm and bench mark this observation, Hsp90-CT was treated with 5 mM novobiocin or with drug vehicle. Hsp90-CT was susceptible to trypsinolysis in the absence of novobiocin (Figure 21, lane 2, 3, 4). However, Hsp90-CT assumed a protease-resistant conformation in the presence of novobiocin (Figure 21, lane 6, 7, 8). This experiment confirmed that novobiocin binds to the carboxy terminus of Hsp90 and that binding of novobiocin to Hsp90-CT and induced a protease-resistant conformation change in Hsp90.

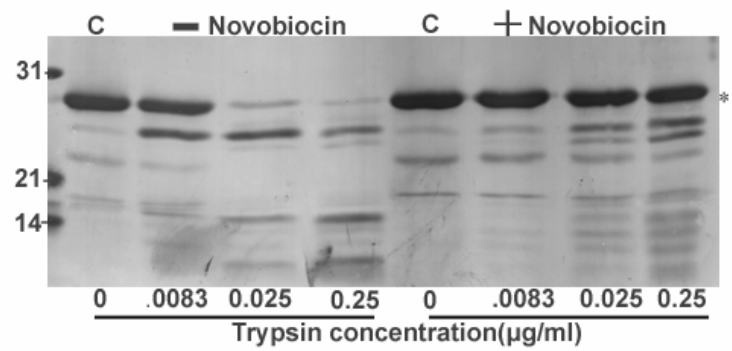


Figure 21: Novobiocin alters conformation of C-terminal domain of Hsp90: Purified recombinant Hsp90-CT was incubated with novobiocin (5mM) or with drug vehicle (DMSO) for 30 minutes on ice. The reactions were then incubated for 6 minutes in presence of indicated concentrations of trypsin and analyzed by Coomassie-stained SDS-PAGE.

Epigallocatechin gallate protects Carboxy terminus of Hsp90 from cleavage by trypsin

To test the hypothesis that epigallocatechin gallate similarly alters the conformation of Hsp90's isolated C-terminal domain, Hsp90-CT was treated with 2 mM epigallocatechin gallate or drug vehicle (DMSO). Hsp90-CT was resistant to proteolysis in the presence of 2 mM epigallocatechin gallate (Figure 22, lane 2, 3, 4). This suggests that epigallocatechin gallate binds to the carboxy terminus of Hsp90. The binding of epigallocatechin gallate enforced a protease-resistant conformation on Hsp90.

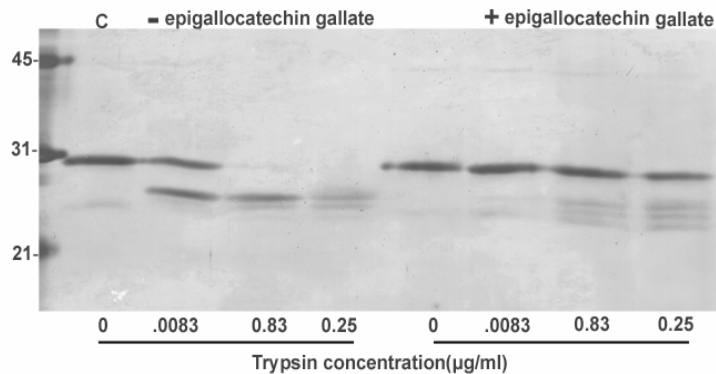


Figure 22: Epigallocatechin gallate alters conformation of C-terminal domain of Hsp90. Purified recombinant Hsp90-CT was incubated with epigallocatechin gallate (2mM) or with drug vehicle (DMSO) for 30 minutes on ice. The reactions were then incubated for 6 minutes in presence of indicated concentrations of trypsin and analyzed by Coomassie-stained SDS-PAGE.

Curcumin protects carboxy terminus of Hsp90 from cleavage by trypsin

To test the hypothesis that curcumin enforces a protease-resistant conformation on the C- terminal domain of Hsp90, Hsp90-CT was treated with 1 mM curcumin or with drug vehicle (DMSO). In the absence of curcumin, Hsp90-CT was susceptible to trypsinolysis (Figure 23, lane 2, 3, 4). In contrast, curcumin was able to enforce a protease-resistant conformation on Hsp90-CT (Figure 23, lane 6, 7, 8). This suggests that curcumin binds to the carboxy terminus of Hsp90.

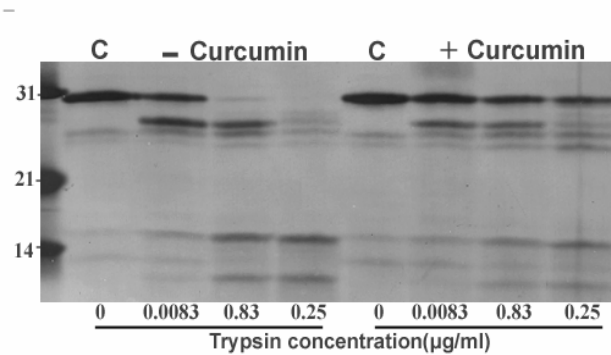


Figure 23: Curcumin alters the conformation of C-terminal domain of Hsp90.

Purified recombinant Hsp90-CT was incubated with curcumin (1mM) or with drug vehicle (DMSO) for 30 minutes on ice. The reactions were then incubated for 6 minutes in presence of indicated concentrations of trypsin and analyzed by Compassion-stained SDS-PAGE.

CHAPTER-IV

DISCUSSION

In my work, I found that novobiocin, epigallocatechin gallate and curcumin inhibit Hsp90 function. In rabbit reticulocyte model system (RRL), denovo folding and maturation of Lck requires Hsp90 activity (46). Using this assay, my results indicate that novobiocin, epigallocatechin gallate and curcumin inhibit Hsp90, leading to production of Lck molecules which are deficient in kinase activity. Densitometric analysis of two assays suggests that epigallocatechin gallate, curcumin, novobiocin, and geldanamycin inhibit the Hsp90-mediated activation of Lck by 33%, 67%, 83%, 99%, respectively (Figure 8). However, more repeats would help us to validate this conclusion statistically.

Under the assay conditions used in Figure 9, I found that novobiocin, curcumin, epigallocatechin gallate do not inhibit Lck directly. When these drugs are added to RRL containing *mature* Lck immediately before immunoadsorption, they do not compromise the phosphotransferase activity of Lck subsequently assayed in the presence of millimolar concentrations of ATP. This suggests that in the presence of high concentrations of ATP, the kinase has a higher affinity for ATP than remaining traces of drugs, demonstrating that the drug effects are not mediated due to their direct binding to Lck. Under the assay Conditions used in figure 8, 9. However, when novobiocin, epigallocatechin gallate and curcumin are added directly to Lck assays containing micromolar concentrations of ATP, these drugs inhibit Lck directly, suggesting that novobiocin, curcumin, epigallocatechin gallate may compete with ATP for binding to kinase, leading to an inhibition of kinase

activity. This suggests that these drugs can have two different mechanisms when assayed under different conditions. The possible ability of novobiocin, curcumin and epigallocatechin gallate to compete with the ATP-binding site on Lck suggest that in future assays an alternate substrate for Hsp90, lacking an ATP binding domain, would be best suited to clearly determine the ability of these drugs to impair Hsp90's chaperoning ability.

Curcumin, epigallocatechin gallate and novobiocin have similar effects on the interaction of Lck with Hsp90 and its co-chaperones. Geldanamycin- and novobiocin-inhibited Hsp90 function by 99%, 83% respectively (Figure 8B, lane 6, 5), while disrupting the association of Hsp90 and Cdc37 with Lck by 97.5% and 98% respectively (Figure 10B, lane 6, 5). However, curcumin and epigallocatechin gallate inhibit Hsp90 function by 67% and 33% respectively (Figure 8B, lane 3, 4) without entirely disrupting the association of Hsp90 and Cdc37 with Lck (63% and 41%, respectively), (Figure 10B, lane 3, 4). Comparing Hsp90 inhibition versus disruption, I found that these drugs have a co-related effect between the efficiency to inhibit and disrupt the complex formation between Lck and Hsp90 and Cdc37. These results suggest that these drugs could have similar effects on Hsp90's interaction with Lck, however, the inability of curcumin and epigallocatechin gallate to completely disrupt the interaction of Lck interaction with Hsp90 and Cdc37 could suggest that curcumin and epigallocatechin gallate are quantitatively less efficient in inhibiting Hsp90-mediated activation of Lck and also in disrupting the interaction of Hsp90 and Cdc37 with Lck when compared to novobiocin and geldanamycin.

Under the assay conditions used in Figure 9, I was surprised to find that matured Lck remained associated with Cdc37 and Hsp90. This contradicts previous work showing that matured Lck molecules are free of Hsp90 and its co-chaperones. One possibility is that drug binding to mature Lck leads to the disruption of the native structure of Lck, which in turn invites Hsp90-mediated chaperone activity to refold Lck to its native conformation. However, control reactions with 1% DMSO, also showed the prolonged or continued interaction of Lck with Hsp90 and Cdc37, arguing that DMSO might alter the native structure of Lck. However, the inability of geldanamycin to disrupt the interaction of Lck with Hsp90 and Cdc37, suggest that the drug-mediated effects are not chaperone-related. As another possibility, phosphorylation of Cdc37 in complexes with v-Src kinase was reported by Brugge et al. (54). Thus, Lck might mediate the phosphorylation of Cdc37. SH2 domain of Lck might then bind the phosphorylated Cdc37.

A single binding site for novobiocin has been postulated to reside in the C-terminal domain of Hsp90 (35, 36 B, 38). Crystal structures of C-terminal domain of *E. coli* Hsp90 homolog HtpG show a possible binding pocket for novobiocin (Figure 2). The helices 3, 4, 5 lines up this binding pocket. Based on the crystal structure, Allan et al (47). used point mutations and identified a possible binding site of novobiocin which overlaps with the hydrophobic region in C-terminal half of helix 4 and a part of helix 5 (Residue 645-673 or human Hsp90 β). The crystal structure also demonstrates that helix 2 has a highly flexible loop containing amino acids ANMERIMKA. Allan et al. (47) speculate that the binding of coumarin antibiotics promotes the repositioning of helix 2.

Consistent with these reports, I found evidence that C-terminal domain of Hsp90 has a site for novobiocin binding. Binding of novobiocin to the C-terminal domain of

truncated Hsp90 induces a protease-resistant conformation. This demonstrates that C-terminal domain of Hsp90 has a binding site for novobiocin (Figure 21). Similarly, epigallocatechin gallate also induced a protease-resistant conformation on the C-terminal domain of truncated Hsp90 (Figure 22). This suggests that the C-terminal domain of truncated Hsp90 has a binding site for epigallocatechin gallate. Curcumin, like novobiocin and epigallocatechin gallate, alters the conformation of the C-terminal domain of truncated Hsp90, suggesting that the C-terminal domain of Hsp90 has a binding site for curcumin (Figure 23).

Based on crystal structure and reports by Allan et al. (47), I hypothesize that binding of these drugs to the hydrophobic cleft encompassing helix 4, helix5 of Hsp90 causes the flexible helix 2 containing the “ANMERIMKA” to interact with the drugs. This causes conformational change on ANMERIMKA motif which then forms a cap like structure over the binding site.

The ability of novobiocin, epigallocatechin gallate and curcumin to interfere with the chaperoning function of full length Hsp90 prompted us to investigate whether these drugs inhibit Hsp90 function by inhibiting ATP-mediated conformational switching of full length Hsp90. The Hsp90 inhibitors geldanamycin and molybdate have opposing effects on Hsp90's ATP-dependent interaction with substrates. Molybdate stabilizes the interaction of Hsp90 with clients such as luciferase, Lck, HRI (46) and steroid hormone receptors (47in hartson 99). Molybdate locks Hsp90 in its closed conformation, leading to the interaction of substrates via salt-resistant interactions (46). In contrast, geldanamycin-treated Hsp90 does not interact strongly with its client proteins. Order-of-addition experiments show that geldanamycin prevents the molybdate-enforced binding

of Hsp90 with clients. However, when applied after molybdate, geldanamycin does not reverse the molybdate-induced interaction between Hsp90 and luciferase. These effects show that molybdate and geldanamycin have opposing effects on ATP-mediated chaperoning function of Hsp90.

Similarly, geldanamycin and molybdate have opposing effects on Hsp90's conformation. Proteolytic-fingerprinting assays exploit molybdate, an analog of phosphate in ATP hydrolysis. This conformational change induced by molybdate enforces a protease-resistant conformation on the C-terminal domain of Hsp90 (46). However, geldanamycin has no noticeable effect on Hsp90's fingerprint, suggesting that geldanamycin-bound Hsp90 represents Hsp90 in its native state. Order-of-addition experiments demonstrate that when geldanamycin is added prior to molybdate, it inhibits molybdate from enforcing a proteolytic-resistant Hsp90 conformation. Because geldanamycin competes with ATP for binding to Hsp90 (24, 27), Hsp90's molybdate-mediated conformational change is ATP-dependent, consistent with the postulated role of molybdate as a Pi analog. The inability of molybdate to enforce a proteolytic-resistant conformation on the isolated recombinant C-terminal domain of Hsp90, which lacks the N-terminal ATP-binding domain of Hsp90, also demonstrates that molybdate binding is ATP-mediated. Therefore, molybdate binding is thought to induce conformational changes on Hsp90 representing Hsp90 in its ATP, [ADP~P~H₂O] or ADP.Pi conformation.

Consistent with previous observations, I observed that molybdate binding enforces the protease-resistance within the C-terminal domain of full-length Hsp90 (Figure 12, lane 3). I also found that in order-of-addition experiments, geldanamycin-

and molybdate bound conformations are not freely exchangeable in the presence of 20 mM molybdate. In contrast to previous reports, however, I found that in the presence of 5 mM molybdate, geldanamycin was able to slightly *reverse* the molybdate-induced conformational of Hsp90 (Figure 12, lane 5). This suggests that at low concentrations of molybdate, molybdate enforces a protease-resistant conformation which is in equilibrium with ADP and nucleotide-free conformations of Hsp90. Addition of geldanamycin shifts the reaction cycle towards a dead-end complex, thereby inhibiting molybdate effects on Hsp90.

The ATP-dependent conformational changes on Hsp90 and the effect of geldanamycin and molybdate on the ATPase cycle are modeled in Figure 24. In the beginning of the reaction cycle, Hsp90 exists in equilibrium between its ATP, ADP and nucleotide-free states (Step 1, 2, and 5 of Figure 24).

In step 3 of the reaction cycle, Hsp90 is represented in its intermediate state of ATP hydrolysis [ADP~P~H₂O]. This induces a proteolytic-resistant conformation on the C-terminal domain leading to the structuring of the flexible ANMERIMKA motif.

In step 4 of the reaction cycle, ATP hydrolysis produces the ADP.Pi bound conformation. Release of Pi from ADP causes an empty binding pocket for Pi, as represented in step 5 of reaction cycle. The binding and release of Pi is a reversible process.

In the presence of molybdate, molybdate occupies the empty Pi binding pocket on Hsp90 (reaction step 6 of Figure 24). Molybdate binding locks Hsp90 in its closed form, also locking ADP in its N-terminal pocket and preventing Hsp90 from undergoing its ATPase cycle. Binding of molybdate also causes the structuring of ANMERIMKA motif.

In the presence of low concentration of molybdate, binding and release of molybdate to ADP and ADP.MoO₄ bound conformation is a reversible process. However, in the presence of higher concentration of molybdate, Hsp90 is locked in its molybdate-bound conformation as represented in step 6 of reaction cycle. This leads to molybdate-dependent reversibility of step 5, 6 of Figure 24). In step 7 of Figure 24, Hsp90 is shown in its geldanamycin bound conformation. Binding of geldanamycin (17 μ M) causes a dead-end complex formation, whereby Hsp90 is locked in its open conformation by preventing ATP binding. The formation of dead-end complex leads to irreversibility between geldanamycin and nucleotide-free Hsp90 conformation.

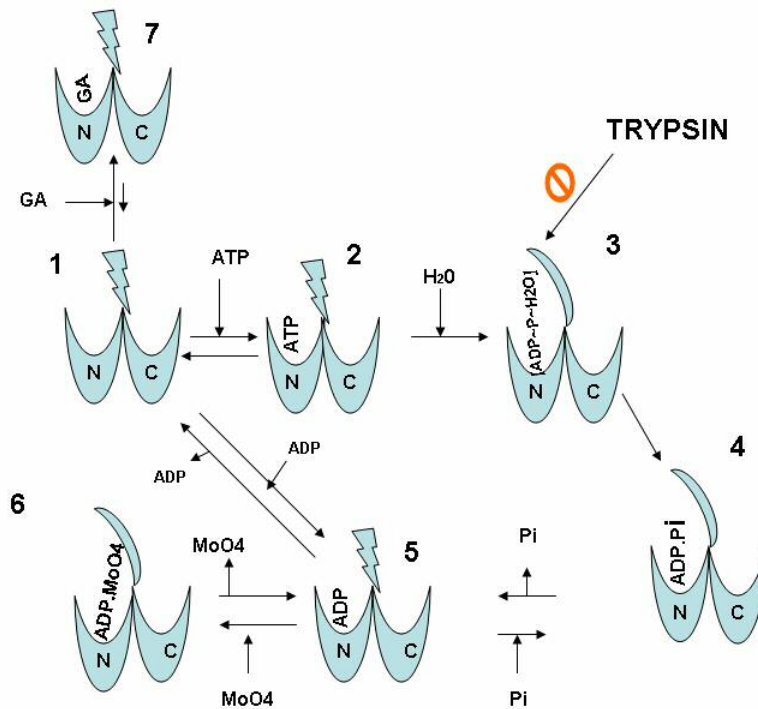


Figure 24: Effect of molybdate and geldanamycin on Hsp90 ATPase cycle

In my assays, I observed that novobiocin can have a mechanism of action distinct from molybdate. Novobiocin could reverse the molybdate-induced structuring of the C-terminal domain of full-length Hsp90 (Figure 13, lane 4). Similarly, the ability of novobiocin to induce a proteolytic-resistant conformation on isolated C-terminal domain of Hsp90 suggests that novobiocin has a mechanism of action distinct from molybdate (Figure 21), because molybdate-induced conformational changes are dependent on binding of ATP to N-terminal domain. Furthermore, 5 mM novobiocin did not structure the full length-Hsp90's itself (Figure 13, lane 4). The ability of novobiocin to reverse molybdate-induced conformational switching of Hsp90, suggest that novobiocin can have a mechanism of action different from molybdate (Figure 13, lane 5).

However, Yun et al. suggested that novobiocin structures full-length Hsp90 and that molybdate and novobiocin induces conformational changes via cooperative mechanism. They observed that in the presence of 20 mM molybdate, 0-5 mM novobiocin was able to potentiate molybdate-induced conformational changes. In my assays however, molybdate-induced switching of Hsp90 conformation can be inhibited or reversed by novobiocin.

This inconsistency can be attributed to the difference in molybdate and novobiocin concentrations used in the two studies. In my assays, 5 mM molybdate is sufficient to induce a proteolytic-resistant conformation on the full length Hsp90, compared to 20 mM molybdate used by Yun et al. Consistent with Yun et al, I also found that at the 20 mM higher concentration, molybdate-induced conformational changes on Hsp90 are potentiated by 5 mM novobiocin. However, I found in my assays that

increasing the novobiocin concentration above 5 mM yields an entirely different picture. At higher novobiocin concentration novobiocin begins to reverse the molybdate-induced conformational changes on Hsp90. (see Figure 25).

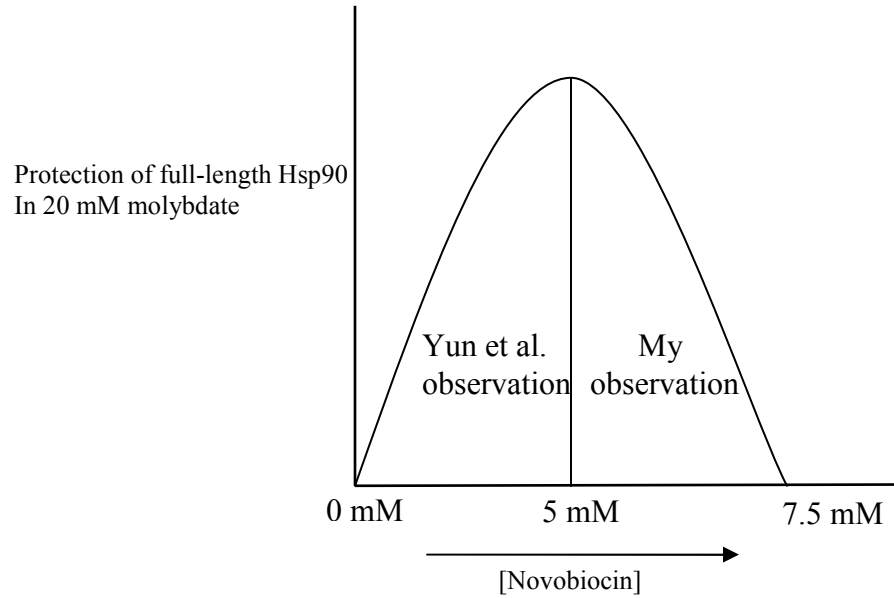


Figure 25: Novobiocin mediates conformational changes on Hsp90.

Molybdate induced conformational changes on Hsp90 are potentiated in the presence of novobiocin. However, novobiocin at a concentration greater than 5 mM reverses molybdate-induced conformational change on Hsp90.

Novobiocin's ability to both potentiate molybdate-induced conformational changes on full-length Hsp90 and also to reverse the molybdate-induced conformational changes on full-length Hsp90 suggests a model of action for these two compounds. (Figure 14). In the 1st step of the reaction cycle, Hsp90 is present in its default conformation. In the default conformation, as mentioned earlier, the binding and release of ADP is a reversible process.

In the 2nd step of the reaction cycle, the presence of high concentration of molybdate causes Hsp90 to assume an ADP.MoO₄ bound conformation. This enforces a structural conformation on the ANMERIMKA motif present in the C terminal domain of Hsp90 (Figure 13). The 1st and the 2nd step of the reaction cycle are in equilibrium and hence are reversible. High concentration of molybdate shifts the reaction cycle to the right-hand side strongly enforcing protease-resistant conformation on the C-terminal domain of full-length Hsp90.

In the presence of low concentrations of molybdate, Hsp90 assumes a proteolytic-resistant conformation (step 1, 2 of Figure 26). Low concentrations of novobiocin potentiate re-structuring of the ANMERIMKA motif induced by molybdate (curve 1 of Figure 23). However, increasing the concentration of novobiocin brings novobiocin concentration high enough to match the affinity for the N- terminal binding site of Hsp90 (Step 4, 5 of Figure 26). Now novobiocin competes with ATP for binding to the N-terminal binding site of Hsp90. Binding of novobiocin to the N-terminal domain of Hsp90, like geldanamycin prevents ADP and molybdate from enforcing a conformational change on the C-terminal domain of Hsp90, as molybdate-induced conformational change is ATP dependent. This suggests that novobiocin has two different binding sites

on Hsp90. A high affinity binding site at the C-terminal domain of Hsp90 and a low affinity site at the N-terminal domain of Hsp90.

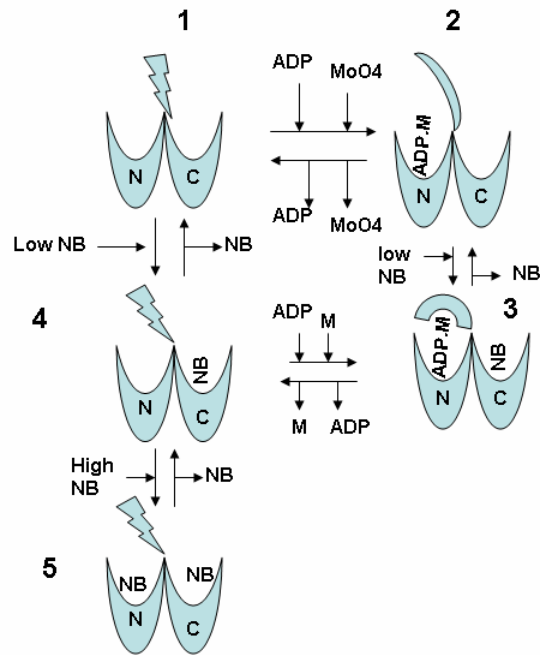


Figure 26: Effect of molybdate and novobiocin on Hsp90-ATPase cycle

In my assays I observed that epigallocatechin gallate can have a mechanism of similar to novobiocin. Like novobiocin, epigallocatechin gallate also could reverse the molybdate-induced structuring of the full length Hsp90 (Figure 15, lane 3). Like novobiocin, epigallocatechin gallate also induces a proteolytic-resistant conformation on isolated C-terminal domain of Hsp90 (Figure 22). These results suggest that novobiocin and epigallocatechin gallate could share the same mechanism of action.

Epigallocatechin gallate was used only at high concentration (5 mM). However, it would be interesting to see if epigallocatechin gallate like novobiocin would potentiate the molybdate-induced conformational changes on full-length Hsp90 when used at a low concentration. It would also be of great interest to know that whether novobiocin and epigallocatechin gallate could compete for the same binding site. These assays would reveal if both novobiocin and epigallocatechin gallate share the same mechanism of action and probably the same site of action.

The inability of curcumin to induce a conformational change on the C-terminal domain of full-length Hsp90 suggests that it might have a mechanism similar to geldanamycin (Figure 23). However, the inability of curcumin to inhibit molybdate-induced conformational changes on the full-length Hsp90 suggest that 1 mM curcumin does not compete with ATP for binding to nucleotide binding site on N-terminal domain of full-length Hsp90 (Figure 16, lane 3). Similarly, curcumin could not prevent geldanamycin's opposition to molybdate-induced conformational change on C-terminal domain of full-length Hsp90, demonstrating that curcumin does not have any effect on the conformation of Hsp90.

The inability of curcumin to inhibit or duplicate geldanamycin effects clearly suggests that both these drugs do not compete (Figure 17, lane 4).

Similarly, curcumin does not seem to share the same site and mechanism of action with novobiocin and epigallocatechin gallate. Curcumin could not prevent epigallocatechin gallate's ability to reverse molybdate-induced conformational changes on C-terminal domain of full-length Hsp90 (Figure 18, lane 5). Curcumin could not prevent novobiocin's ability to restructure the C-terminal domain of full-length Hsp90 (Figure 19, lane 4). This suggests that curcumin has a unique site of action compared to epigallocatechin gallate and novobiocin.

However, in these assays, curcumin (1 mM) is used at a low concentration under these assay conditions, compared to epigallocatechin gallate (5 mM) and molybdate (5 mM). Curcumin (1 mM) was sufficient to induce a protease-resistant conformation on recombinant C-terminal domain of Hsp90. So I used curcumin in the same concentration to study its effect on full-length Hsp90. This raises the possibility that inability of curcumin to reverse molybdate-induced conformational changes on C-terminal domain of full-length Hsp90 could be due to low concentration used in this assay. Moreover, the inability of curcumin to prevent epigallocatechin gallate from inducing conformational changes on the C-terminal domain of full-length Hsp90 also could also be attributed to lack of competitive inhibition between epigallocatechin gallate and curcumin. In future, experiments with similar concentration of curcumin and epigallocatechin gallate would help us to clearly predict if these drugs share the same binding site. Isothermal calorimetry would certainly help us in determining K_d for these drugs.

Together this study characterizes new flagship inhibitors of Hsp90 function. However, since high concentration of drugs was used in all these assays, it is not conclusive whether these drugs would be a specific inhibitors used *in vivo* at physiologically relevant concentrations. Interestingly, these drugs have the ability to alter the structural conformation of Hsp90, suggesting these drugs would of immense help in understanding the ATPase cycle of Hsp90. Future studies on these compounds could provide deep insight on function of Hsp90.

CHAPTER V

INTRODUCTION

Novobiocin binds to the carboxy terminus of Hsp90

Previous experiments with recombinant chicken Hsp90 show Hsp90 bind to novobiocin-sepharose. Similarly, binding of C-terminal domain of Hsp90 to ATP-Sepharose resin is inhibited by novobiocin or soluble ATP, suggesting that both novobiocin and ATP bind to same site on C-terminal domain of Hsp90 (35). Yun et al. (37) observed that novobiocin induces conformational changes in C terminal domain of Hsp90. These observations confirm the ability of Hsp90 to bind novobiocin. However, Since novobiocin and Hsp90 are not covalently bonded, it has been a great difficulty to study the specific peptide in Hsp90 that bind novobiocin. To overcome this difficulty, I will be using photoaffinity novobiocin analogs, which bind to Hsp90 covalently, hence the crosslinked peptide could be identified by MALDI-TOF mass spectrometer.

Novobiocin inhibits co-chaperone binding to Hsp90:

Novobiocin influences Hsp90's co-chaperone binding ability. Hsp90 β pretreated with novobiocin was added to denatured rhodanese and the rate of rhodanese aggregation was studied by monitoring the increase in the light scattering. Rhodanese aggregation increased significantly in the presence of novobiocin. These results suggest the ability of novobiocin to influence the conformation of Hsp90, thereby reducing the co- chaperone binding ability of Hsp90.

MATERIALS AND METHODS

Reagents:

Sinapinic acid (SA) was purchased from Sigma (530-59-6). MALDI-Matrix solutions were prepared fresh as a saturated solution in 30% acetonitrile and 0.1% trifluoroacetic acid.

Photolabile novobiocin analogs (*KU-24*, *KU-25*, *KU-26*, and *KU-27*) were provided by Dr. Brian J Blagg, University of Kansas. These analogs have phenolic ring of novobiocin replaced by phenylazide group (Figure 27). The recombinant carboxy-terminal domain of Hsp90 was expressed and purified in *E. coli* as described in Chapter 2.

UV crosslinking

Hsp90 CT (~25µg) or apomyoglobin were mixed with 5 mM of each novobiocin analogs in a 15 µl reaction containing assay buffer (10 mM Tris HCl pH7.4, 150 mM NaCl, 4 mM CaCl₂, 0.1 mM EDTA). The reactions were incubated at room temperature for 10 minutes. After incubation, reactions were placed on a clean microscopic slide and subjected to moderate photo exposure (1-4 flashes with a camera flash bulb) or to UV. UV crosslinking was carried out on a Stratagene UV Stratalinker 1800 with 254 nm bulbs. The samples were placed 7 cm from the UV bulbs. The power of the instrument was set at 184 µJ. The samples were exposed one to four times with the instrument set at 184 µJ per exposure. After each exposure, aliquots (1.5µl) of the reaction mixed with matrix and then spotted on an MALDI plate and allowed to dry. After drying, samples were loaded on MALDI-TOF mass spectrometer. The spectra were obtained using on Applied Biosystems Voyager-DE Pro MALDI-TOF mass spectrometer operated in the linear mode. A total of 500 single spectra (50 X 10 TOF analyses) were accumulated.

The parameters used were: grid voltage 91%, guide wire 0.05%. The detector gating was set to 1000 kDa.

Structure of Photoaffinity analogs of novobiocin:

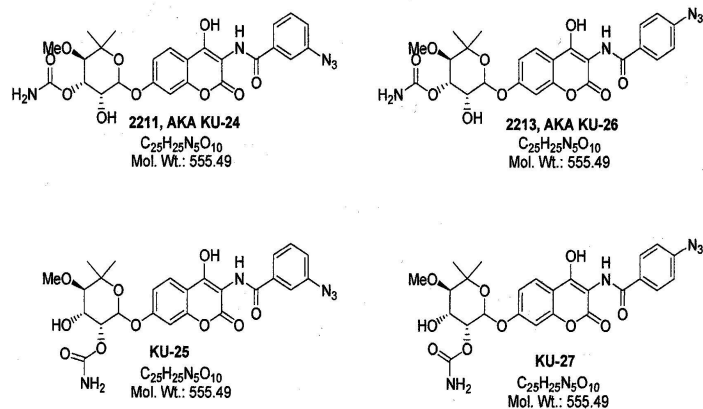


Figure 27: Structure of photoaffinity analogs of novobiocin. Photoaffinity analogs of novobiocin: (Structure and compound courtesy Dr. Brian J Blagg, (University of Kansas)).

RESULTS

Photoexposure of novobiocin to Hsp90-CT

To determine if specific crosslinking could be achieved between Hsp90-CT and novobiocin, Hsp90-CT was mixed with 5 mM of novobiocin, exposed to one modest dose of UV (184 μ J) and analyzed by MALDI-TOF mass spectrometry. The theoretical mass for Hsp90-CT is 24580, while the observed mass is ~150 m/z higher than theoretical mass. This observed error in mass of Hsp90-CT is because the spectra were obtained with default instrument calibration without external or internal standards.

MALDI-TOF analysis showed Hsp90-CT species with an apparent addition of ~+200 m/z representing a typical matrix adduct. Controls indicated that neither novobiocin nor UV alone altered Hsp90-CT mass. (Figure 28, A, B). Similarly, a combination of UV and novobiocin did not alter Hsp90-CT mass, suggesting novobiocin was unable to crosslink with Hsp90-CT (Figure 28, C).

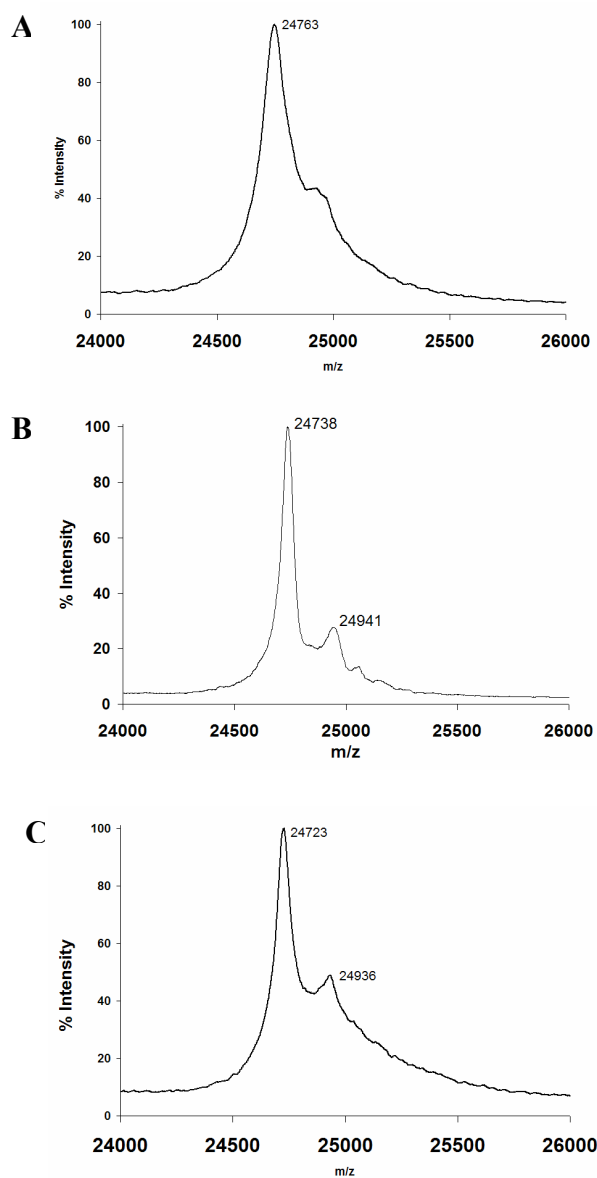


Figure 28: Photo exposure of novobiocin and Hsp90-CT. Hsp90-CT analyzed by MALDI-TOF mass spectrometry after (A) UV exposure (B) treatment with novobiocin, (C) simultaneous treatment with novobiocin and UV.

Photoaffinity analogs:

The inability of novobiocin to crosslink with Hsp90-CT upon UV exposure, suggest the non-covalent interaction between Hsp90-CT and novobiocin. The inability of novobiocin to covalently bond to Hsp90-CT prompted us to use photoaffinity novobiocin analogs, which have phenylazide group replacing phenolic group of novobiocin. The phenylazide group upon UV or light exposure forms a nitrene group that can insert to C-H or N-H site on protein. To first determine if that the photo affinity analogs of novobiocin bind to Hsp90, Hsp90-CT was treated with 5 mM novobiocin analog (*KU-26*) or with drug vehicle. Hsp90-CT was susceptible to trypsinolysis in the absence of analog (Figure 29, lane 1-4), but Hsp90-CT assumed a protease-resistant conformation in the presence of analog (Figure 29, lane 5-8). This protection demonstrated that novobiocin analog *KU-26* binds to the carboxy- terminus of Hsp90.

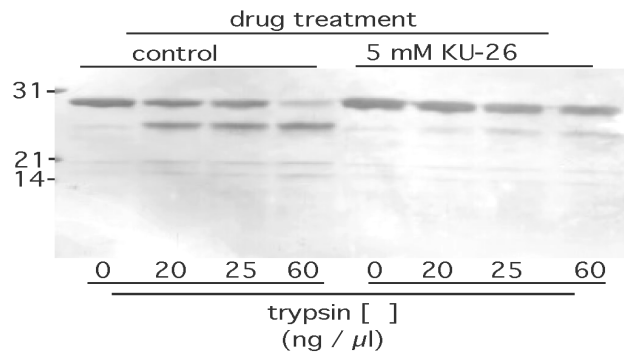


Figure 29: Novobiocin analog *KU-26* alters the conformation of Hsp90-CT. Hsp90-CT was incubated with novobiocin analog (5 mM *KU-26*) or with drug vehicle (DMSO), for 30 minutes on ice. The reactions were then incubated for 6 minutes in presence of indicated concentrations of trypsin, analyzed by SDS-PAGE, and stained with Coomassie blue.

Photoexposure (UV) of Hsp90-CT and KU-26

To determine if specific crosslinking could be achieved between Hsp90-CT and analog *KU-26*, Hsp90-CT was mixed with 5 mM *KU-26*, exposed to modest dose of UV (184 μ J) and analyzed by MALDI-TOF mass-spectrometry. MALDI-TOF analysis of the control reaction confirmed that UV itself did not induce any crosslinking (Figure 30A). UV exposure of Hsp90-CT to *KU-24* generated a new Hsp90-CT species mass with an apparent addition of ~ 540 m/z to the parental mass suggesting the covalent crosslinking of *KU-24* to Hsp90-CT (Figure 30B).

Other analogs

To determine the ability of other analogs to crosslink specifically to Hsp90-CT, Hsp90-CT was mixed with 5 mM of *KU-25*, exposed to one modest dose of UV (184 μ J) and analyzed by MALDI-TOF mass-spectrometry (Figure 30C). This resulted in strong crosslinking of one to four molecules of *KU-25* to Hsp90-CT. Crosslinking of *KU-26* showed less efficient crosslinking of one to four drug molecules of *KU-26* to Hsp90-CT (Figure 30D). *KU-27* also showed crosslinking efficiency equal to *KU-26*, weaker than *KU-25* but stronger than *KU-26* (Figure 30E). These results indicate that the position of the azide and carbamyl group affected the crosslinking efficiency (Figure 27).

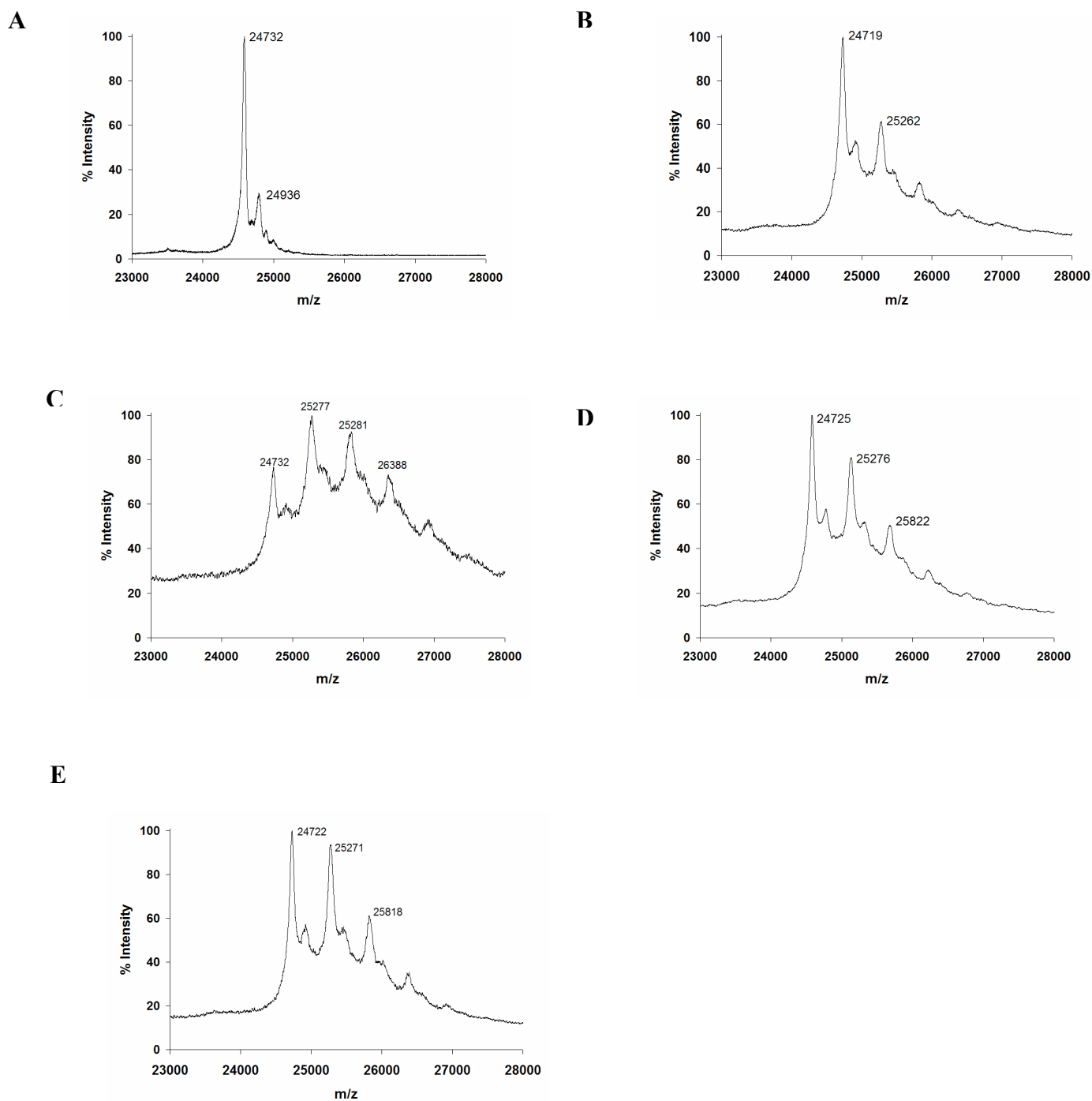


Figure 30: Photoaffinity novobiocin analogs specifically crosslink to the C-terminal domain of Hsp90. Hsp90-CT was incubated with drug or drug vehicle (DMSO) exposed to UV radiation and analyzed by MALDI-TOF mass spectrometry. Spectrum (A) control reactions performed with DMSO, (B) reactions performed with *KU-24*, (C) reactions

performed with *KU-25* (D) reactions performed with *KU-26* (E) reactions performed with
KU-27

Crosslinking of novobiocin analogs to Hsp90-CT is highly specific.

To determine if crosslinking of novobiocin analog to Hsp90-CT is specific, Hsp90-CT was incubated with a mix of both 5 mM novobiocin and 5 mM of novobiocin analog (*KU-26*). Subsequent MALDI-TOF analysis showed most of the crosslinking ability of the analog *KU-26* was inhibited, in the presence of 5 mM novobiocin. (Figure 31A vs. 31B). This demonstrates that the crosslinking of analogs is highly specific to the novobiocin-binding site on Hsp90-CT.

To confirm that crosslinking of novobiocin analogs to Hsp90-CT was specific, an unrelated protein apomyoglobin was incubated with the most potent crosslinking analog *KU-25* and subjected to UV exposure. Subsequent MALDI-TOF analysis failed to reveal apomyoglobin ion with an addition of ~540 m/z to the parental mass, demonstrating that crosslinking is specific to Hsp90-CT (Figure 31C) and was not due to non-specific interactions or events.

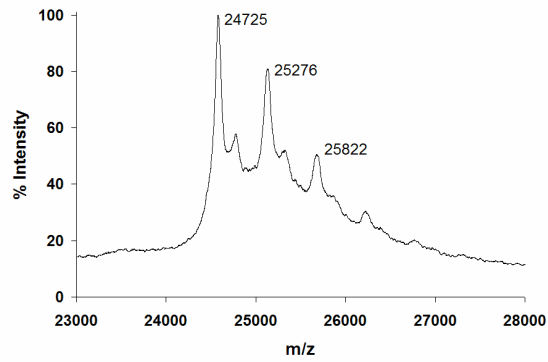
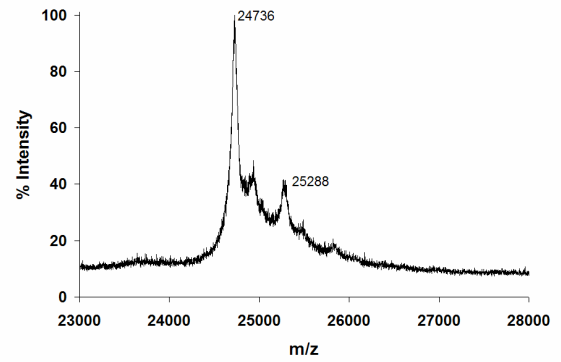
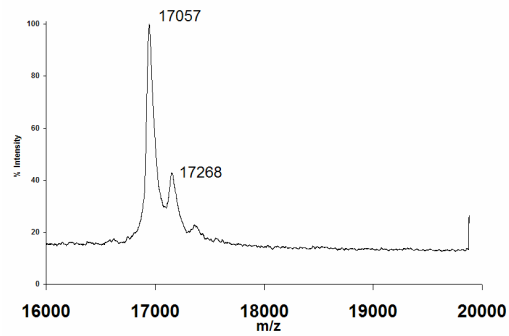
A**B****C**

Figure 31: Crosslinking of Novobiocin analogs is highly specific. Purified proteins were exposed to UV in the presence of *KU-26* and subsequently analyzed by MALDI-TOF mass spectrometry. (A) Hsp90-CT (B) Hsp90-CT with *KU-26* and 5 mM of competing soluble novobicin (C) apomyoglobin.

DISCUSSION

The photoaffinity novobiocin analog *KU-26* binds to the C-terminal domain of recombinant Hsp90-CT (Figure).

MALDI-TOF analysis of the crosslinking between analogs *KU-24*, *KU-25*, *KU-26*, *KU-27* and Hsp90-CT in the presence of modest dose of UV demonstrated new species of Hsp90-CT with an apparent addition of ~540 m/z (Figure 30). However, the theoretical molecular weight of photoaffinity analogs is 555.49. The observed mass difference is 15 Da. The chemistry of phenylazide crosslinking which typically leads to loss of two nitrogen atoms. Thus, the mass difference should be 527 Da after crosslinking. However, I observed a difference of 540 Daltons. This could be due to the addition of water molecules and ring rearrangements after the crosslinking event. However, the mass accuracy of my spectrum, the difference in molecular weight difference hence cannot be explored in detail.

The crosslinking of photoaffinity analogs to Hsp90-CT is highly specific. The inability of these analogs to crosslink to an unrelated protein (apomyoglobin) (Figure 31C), suggest that the crosslinking is highly specific to Hsp90-CT. Competition studies shows the crosslinking of *KU-26* to Hsp90-CT reduced by ~70% in presence of soluble novobiocin, demonstrating that both soluble novobiocin and *KU-26* compete for the same binding site on Hsp90-CT (Figure 31B).

The different photoaffinity analogs exhibit different efficiencies in crosslinking to Hsp90-CT (Figure 30A-E). These results suggest that each analog has different efficiency in crosslinking to Hsp90-CT. The presence of carbamyl group acts as a major force in driving multiple crosslinking. Even though, *KU-24* and *KU-25* differ structurally

only at the position of carbamyl group and its neighboring hydroxyl group, they show a substantial difference in crosslinking efficiency (Figure 24). Similarly, *KU-26* and *KU-27* also differ structurally only at position of hydroxyl and its neighboring carbamyl group, yet they shown a marked difference in crosslinking efficiency. These results suggest that the carbamyl group plays a major role in high affinity binding to Hsp90-CT.

Similarly, the presence of azide group in the meta position potentiates crosslinking. Crosslinking efficiency of *KU-25* versus *KU-27* shows that because *KU-27* differs from *KU-25* only in the positioning of nitrene group at ortho position, only two molecules of *KU-27* crosslinks compared to four by *KU-25*. Crosslinking efficiency of *KU-24* versus *KU-26* does not show a significantly efficient crosslinking, even though *KU-24* like *KU-25* has an azide group in meta position. This shows that both the nitrene and carbamyl group positioning plays a major role in high affinity binding to Hsp90-CT. In our studies we have shown that novobiocin binds to Hsp90, and that novobiocin analogs could be crosslinked to Hsp90. Future works focusing site of novobiocin crosslinking would help us to get a better insight of structure and functional relationships between novobiocin and Hsp90.

BIBLIOGRAPHY

1. Sullivan, W., et al., *Nucleotides and two functional states of hsp90*. J Biol Chem, 1997. **272**(12): p. 8007-12.
2. Dobson, C.M. and M. Karplus, *The fundamentals of protein folding: bringing together theory and experiment*. Curr Opin Struct Biol, 1999. **9**(1): p. 92-101.
3. Vendruscolo, M., et al., *Protein folding and misfolding: a paradigm of self-assembly and regulation in complex biological systems*. Philos Transact A Math Phys Eng Sci, 2003. **361**(1807): p. 1205-22.
4. Anfinsen, C.B., *Principles that govern the folding of protein chains*. Science, 1973. **181**(96): p. 223-30.
5. Dill, K.A. and H.S. Chan, *From Levinthal to pathways to funnels*. Nat Struct Biol, 1997. **4**(1): p. 10-9.
6. Radford, S.E. and C.M. Dobson, *From computer simulations to human disease: emerging themes in protein folding*. Cell, 1999. **97**(3): p. 291-8.
7. Radford, S.E., *Protein folding: progress made and promises ahead*. Trends Biochem Sci, 2000. **25**(12): p. 611-8.
8. Dobson, C.M., *Protein misfolding, evolution and disease*. Trends Biochem Sci, 1999. **24**(9): p. 329-32.
9. Hesterkamp, T., et al., *Escherichia coli trigger factor is a prolyl isomerase that associates with nascent polypeptide chains*. Proc Natl Acad Sci U S A, 1996. **93**(9): p. 4437-41.
10. Patzelt, H., et al., *Binding specificity of Escherichia coli trigger factor*. Proc Natl Acad Sci U S A, 2001. **98**(25): p. 14244-9.
11. Young, J.C., et al., *Pathways of chaperone-mediated protein folding in the cytosol*. Nat Rev Mol Cell Biol, 2004. **5**(10): p. 781-91.
12. Lindquist, S. and E.A. Craig, *The heat-shock proteins*. Annu Rev Genet, 1988. **22**: p. 631-77.
13. Fedorov, A.N. and T.O. Baldwin, *Cotranslational protein folding*. J Biol Chem, 1997. **272**(52): p. 32715-8.
14. Carrell, R.W. and D.A. Lomas, *Conformational disease*. Lancet, 1997. **350**(9071): p. 134-8.
15. Gething, M.J. and J. Sambrook, *Protein folding in the cell*. Nature, 1992. **355**(6355): p. 33-45.
16. Ruddon, R.W. and E. Bedows, *Assisted protein folding*. J Biol Chem, 1997. **272**(6): p. 3125-8.
17. Smith, D.F., L. Whitesell, and E. Katsanis, *Molecular chaperones: biology and prospects for pharmacological intervention*. Pharmacol Rev, 1998. **50**(4): p. 493-514.
18. Lai, B.T., et al., *Quantitation and intracellular localization of the 85K heat shock protein by using monoclonal and polyclonal antibodies*. Mol Cell Biol, 1984. **4**(12): p. 2802-10.
19. Welch, W.J. and J.R. Feramisco, *Purification of the major mammalian heat shock proteins*. J Biol Chem, 1982. **257**(24): p. 14949-59.

20. Pratt, W.B. and D.O. Toft, *Regulation of signaling protein function and trafficking by the hsp90/hsp70-based chaperone machinery*. Exp Biol Med (Maywood), 2003. **228**(2): p. 111-33.
21. Argon, Y. and B.B. Simen, *GRP94, an ER chaperone with protein and peptide binding properties*. Semin Cell Dev Biol, 1999. **10**(5): p. 495-505.
22. Wearsch, P.A., L. Voglino, and C.V. Nicchitta, *Structural transitions accompanying the activation of peptide binding to the endoplasmic reticulum Hsp90 chaperone GRP94*. Biochemistry, 1998. **37**(16): p. 5709-19.
23. Blachere, N.E., et al., *Heat shock protein-peptide complexes, reconstituted in vitro, elicit peptide-specific cytotoxic T lymphocyte response and tumor immunity*. J Exp Med, 1997. **186**(8): p. 1315-22.
24. Stebbins, C.E., et al., *Crystal structure of an Hsp90-geldanamycin complex: targeting of a protein chaperone by an antitumor agent*. Cell, 1997. **89**(2): p. 239-50.
25. Prodromou, C., P.W. Piper, and L.H. Pearl, *Expression and crystallization of the yeast Hsp82 chaperone, and preliminary X-ray diffraction studies of the amino-terminal domain*. Proteins, 1996. **25**(4): p. 517-22.
26. Huai, Q., et al., *Structures of the N-terminal and middle domains of E. coli Hsp90 and conformation changes upon ADP binding*. Structure, 2005. **13**(4): p. 579-90.
27. Grenert, J.P., et al., *The amino-terminal domain of heat shock protein 90 (hsp90) that binds geldanamycin is an ATP/ADP switch domain that regulates hsp90 conformation*. J Biol Chem, 1997. **272**(38): p. 23843-50.
28. Roe, S.M., et al., *Structural basis for inhibition of the Hsp90 molecular chaperone by the antitumor antibiotics radicicol and geldanamycin*. J Med Chem, 1999. **42**(2): p. 260-6.
29. Prodromou, C., et al., *The ATPase cycle of Hsp90 drives a molecular 'clamp' via transient dimerization of the N-terminal domains*. Embo J, 2000. **19**(16): p. 4383-92.
30. Obermann, W.M., et al., *In vivo function of Hsp90 is dependent on ATP binding and ATP hydrolysis*. J Cell Biol, 1998. **143**(4): p. 901-10.
31. Prodromou, C. and L.H. Pearl, *Structure and functional relationships of Hsp90*. Curr Cancer Drug Targets, 2003. **3**(5): p. 301-23.
32. Louvion, J.F., R. Warth, and D. Picard, *Two eukaryote-specific regions of Hsp82 are dispensable for its viability and signal transduction functions in yeast*. Proc Natl Acad Sci U S A, 1996. **93**(24): p. 13937-42.
33. Sato, S., N. Fujita, and T. Tsuruo, *Modulation of Akt kinase activity by binding to Hsp90*. Proc Natl Acad Sci U S A, 2000. **97**(20): p. 10832-7.
34. Panaretou, B., et al., *Activation of the ATPase activity of hsp90 by the stress-regulated cochaperone aha1*. Mol Cell, 2002. **10**(6): p. 1307-18.
35. Marcu, M.G., et al., *The heat shock protein 90 antagonist novobiocin interacts with a previously unrecognized ATP-binding domain in the carboxyl terminus of the chaperone*. J Biol Chem, 2000. **275**(47): p. 37181-6.
36. Wiech, H., et al., *Hsp90 chaperones protein folding in vitro*. Nature, 1992. **358**(6382): p. 169-70.

37. Harris, S.F., A.K. Shiau, and D.A. Agard, *The crystal structure of the carboxy-terminal dimerization domain of htpG, the Escherichia coli Hsp90, reveals a potential substrate binding site*. Structure, 2004. **12**(6): p. 1087-97.
38. Yun, B.G., et al., *Novobiocin induces a distinct conformation of Hsp90 and alters Hsp90-cochaperone-client interactions*. Biochemistry, 2004. **43**(25): p. 8217-29.
39. Soti, C., A. Racz, and P. Csermely, *A Nucleotide-dependent molecular switch controls ATP binding at the C-terminal domain of Hsp90. N-terminal nucleotide binding unmasks a C-terminal binding pocket*. J Biol Chem, 2002. **277**(9): p. 7066-75.
40. Smith, D.F., et al., *Two FKBP-related proteins are associated with progesterone receptor complexes*. J Biol Chem, 1993. **268**(24): p. 18365-71.
41. Johnson, J.L. and D.O. Toft, *A novel chaperone complex for steroid receptors involving heat shock proteins, immunophilins, and p23*. J Biol Chem, 1994. **269**(40): p. 24989-93.
42. Carrello, A., et al., *The common tetratricopeptide repeat acceptor site for steroid receptor-associated immunophilins and hop is located in the dimerization domain of Hsp90*. J Biol Chem, 1999. **274**(5): p. 2682-9.
43. Dutta, R. and M. Inouye, *GHL, an emergent ATPase/kinase superfamily*. Trends Biochem Sci, 2000. **25**(1): p. 24-8.
44. Prodromou, C., et al., *Identification and structural characterization of the ATP/ADP-binding site in the Hsp90 molecular chaperone*. Cell, 1997. **90**(1): p. 65-75.
45. Cutforth, T. and G.M. Rubin, *Mutations in Hsp83 and cdc37 impair signaling by the sevenless receptor tyrosine kinase in Drosophila*. Cell, 1994. **77**(7): p. 1027-36.
46. Hartson, S.D., et al., *Hsp90-mediated folding of the lymphoid cell kinase p56lck*. Biochemistry, 1996. **35**(41): p. 13451-9.
47. Hartson, S.D., et al., *Molybdate inhibits hsp90, induces structural changes in its C-terminal domain, and alters its interactions with substrates*. Biochemistry, 1999. **38**(12): p. 3837-49.
48. Allan, R.K., et al., *Modulation of chaperone function and cochaperone interaction by novobiocin in the C-terminal domain of Hsp90: evidence that coumarin antibiotics disrupt Hsp90 dimerization*. J Biol Chem, 2006. **281**(11): p. 7161-71.
49. Bohen, S.P. and K.R. Yamamoto, *Isolation of Hsp90 mutants by screening for decreased steroid receptor function*. Proc Natl Acad Sci U S A, 1993. **90**(23): p. 11424-8.
50. Nathan, D.F. and S. Lindquist, *Mutational analysis of Hsp90 function: interactions with a steroid receptor and a protein kinase*. Mol Cell Biol, 1995. **15**(7): p. 3917-25.
51. Schulte, T.W., et al., *Antibiotic radicicol binds to the N-terminal domain of Hsp90 and shares important biologic activities with geldanamycin*. Cell Stress Chaperones, 1998. **3**(2): p. 100-8.
52. Bergerat, A., et al., *An atypical topoisomerase II from Archaea with implications for meiotic recombination*. Nature, 1997. **386**(6623): p. 414-7.

53. Marcu, M.G., T.W. Schulte, and L. Neckers, *Novobiocin and related coumarins and depletion of heat shock protein 90-dependent signaling proteins*. J Natl Cancer Inst, 2000. **92**(3): p. 242-8.
54. Palermo, C.M., C.A. Westlake, and T.A. Gasiewicz, *Epigallocatechin gallate inhibits aryl hydrocarbon receptor gene transcription through an indirect mechanism involving binding to a 90 kDa heat shock protein*. Biochemistry, 2005. **44**(13): p. 5041-52.
55. Brugge, J., W. Yonemoto, and D. Darrow, *Interaction between the Rous sarcoma virus transforming protein and two cellular phosphoproteins: analysis of the turnover and distribution of this complex*. Mol Cell Biol, 1983. **3**(1): p. 9-19.

VITA

Palgunan Kalyanaraman

Candidate for the Degree of

Master of Science

Thesis: Hsp90: COMMON TARGET FOR DIVERSE ANTIBIOTICS

Major Field: Biochemistry and Molecular Biology

Biographical:

Personal Data: Born in Salem, India, on April 12, 1979, son of V.S. Kalyanarman and Vanaja Kalyanaraman

Education: Graduated from The Hindu Higher Secondary School, Chennai, India in May 1996; received Bachelor of Science from New College, Chennai, India, in May 1999; Obtained Master of Science from University of Madras, Chennai, India in April 2001; Completed the requirements for the Master of Science degree with a major in Biochemistry and Molecular Biology at Oklahoma State University in December 2006

Experience: Employed by Oklahoma State University, Department of Biochemistry and Molecular Biology, as a research assistant, 2004-present.